ACS Synthetic Biology



pubs.acs.org/synthbio
Research Article

# Leveraging Engineered *Pseudomonas putida* Minicells for Bioconversion of Organic Acids into Short-Chain Methyl Ketones

Ekaterina Kozaeva,[§] Manuel Nieto-Domínguez,[§] Kent Kang Yong Tang, Maximilian Stammnitz, and Pablo Iván Nikel*

Cite This: *ACS Synth. Biol.* 2025, 14, 257−272
Read Online

ACCESS | Metrics & More | Article Recommendations | Supporting Information

**ABSTRACT:** Methyl ketones, key building blocks widely used in diverse industrial applications, largely depend on oil-derived chemical methods for their production. Here, we investigated biobased production alternatives for short-chain ketones, adapting the solvent-tolerant soil bacterium *Pseudomonas putida* as a host for ketone biosynthesis either by whole-cell biocatalysis or using engineered minicells, chromosome-free bacterial vesicles. Organic acids (acetate, propanoate and butanoate) were selected as the main carbon substrate to drive the biosynthesis of acetone, butanone and 2-pentanone. Pathway optimization identified efficient enzyme variants from *Clostridium acetobutylicum* and *Escherichia coli*, tested with both constitutive and inducible expression of the cognate genes. By implementing these optimized pathways in *P. putida* minicells, which can be prepared through a simple three-step purification protocol, the feedstock was converted into the target short-chain methyl ketones. These results highlight the value of combining morphology and pathway engineering of noncanonical bacterial hosts to establish alternative bioprocesses for toxic chemicals that are difficult to produce by conventional approaches.

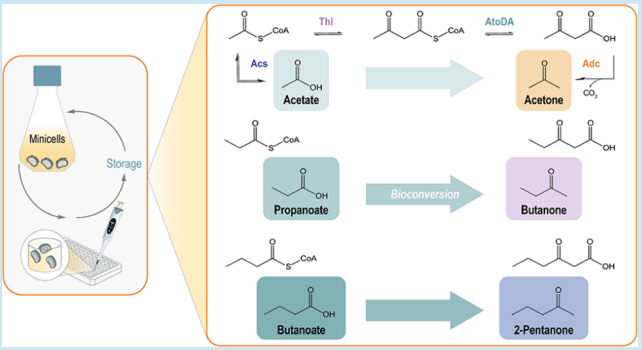


**KEYWORDS:** *metabolic engineering, synthetic biology, Pseudomonas putida, ketones, 2-pentanone, butanone, acetone, minicells*

## INTRODUCTION

Ketones, a class of structurally diverse molecules with the general formula $R-C(=O)-R'$, where $R$ and $R'$ can be a variety of carbon-containing substituents, are currently produced using traditional, oil-based chemistry.[1] Methyl ketones (MKs), a subset of this family of compounds where one ligand on the carbonyl carbon is a $CH_3$ group, play an important commercial role.[2] Because of their strong solvent properties and generally high evaporation rates, ketones are used as building-blocks in the fragrance, flavor, textile, pesticide and agrochemical industries,[3−5] as well as being key precursors for the synthesis of pharma molecules.[6] 2-Pentanone $[CH_3-(CH_2)_2-C(=O)-CH_3]$, a prime example of the broad MK family, has multiple applications in the fragrance sector and it has been recognized as a potent inhibitor of prostaglandin production, associated with colon carcinogenesis.[7] Greener alternatives for ketone production are needed to fulfill the growing market demands, and the adoption of robust microbial cell factories emerges as an attractive option to this end.[8−11] Toxicity issues, imposed on the producer cells by either intermediates or products of solvent biosynthesis pathways, continue to be a major hurdle that impairs the development of stable bioprocesses.[12,13] This occurrence frequently leads to the loss of plasmid(s) encoding components of the biosynthesis pathways or the accumulation of mutations in the genes thereof, resulting in nonproducing phenotypes.[14−16]

Several strategies have been implemented toward extending the lifespan of actively producing cell factories, yet growth-coupled bioprocesses involving harsh, reactive intermediates and products tend to display limited yields due to the stability issues listed above. An alternative approach that can help overcoming such limitations is using anucleated, bacteria-derived vesicles as biocatalysts.[17,18] Chromosome-free minicells, for instance, naturally occur within bacterial populations albeit at very low frequencies.[19] Under normal growth conditions, the *Z* ring constricts and recruits the peptidoglycan synthesis machinery together with its associated proteins.[20] The dynamic assembly of FtsZ units in rod-shaped bacteria is controlled by the Min system, which encompasses the MinC, MinD and MinE structural proteins.[21] MinC and MinD inhibit

**Received:** October 11, 2024
**Revised:** December 13, 2024
**Accepted:** December 17, 2024
**Published:** January 3, 2025

**Table 1. Bacterial Strains and Plasmids Used in This Study**

| Bacterial strain | Relevant characteristics[a] | Reference or source |
|---|---|---|
| *Escherichia coli* | | |
| DH5α λpir | Cloning host; F⁻ λ⁻ *endA1 gln X44*(AS) *thiE1 recA1 relA1 spoT1 gyrA96*(Nal$^R$) *rfbC1 deoR nupG* Φ80(*lacZ*ΔM15) Δ(*argF-lac*)*U169 hsdR17* ($r_K^-$ $m_K^+$), λpir lysogen | Hanahan and Meselson[123] |
| *Pseudomonas putida* | | |
| KT2440 | Wild-type strain; derivative of *P. putida* mt-2 cured of the catabolic TOL plasmid[124] | Bagdasarian et al.[125] |
| SEM1.3 | Reduced-genome derivative of strain EM42;[48] Δ*phaC1ZC2DFI* (Δ*PP_5003-PP_5008*) Δ*benABCD* (Δ*PP_3161-PP_3164*) | Kozaeva et al.[50] |
| SEM1.3 Δ*minD* | Minicell-forming derivative of strain SEM1.3, Δ*minD* (Δ*PP_1733*) | This work |
| KT2440 Δ*minD* | Minicell-forming derivative of strain KT2440, Δ*minD* (Δ*PP_1733*) | This work |

| Plasmid | Relevant characteristics | Reference or source |
|---|---|---|
| pSEVA4413 | Standard vector for constitutive gene expression; $P_{EM7}$ promoter; *oriV*(pRO1600/ColE1); Sm$^R$/Sp$^R$ | Silva-Rocha et al.[63] |
| pS4413-*msfGFP* | Derivative of vector pSEVA4413 for constitutive expression of the monomeric superfolder GFP; $P_{EM7}$→*msfGFP*; Sm$^R$/Sp$^R$ | Fernández-Cabezón et al.[126] |
| pSEVA2313 | Standard vector for constitutive gene expression; $P_{EM7}$ promoter; *oriV*(pBBR1); Km$^R$ | Wirth et al.[127] |
| pS2313-MKc | Derivative of vector pSEVA2313 harboring the genes encoding the canonical acetone biosynthesis pathway from *Clostridium acetobutylicum*; $P_{EM7}$→*thl*$^{Ca}$*ctfAB*$^{Ca}$*adc*$^{Ca}$; Km$^R$ | This work |
| pS2313-MKs1 | Derivative of vector pSEVA2313 harboring the genes encoding a synthetic MK biosynthesis pathway; $P_{EM7}$→*thl*$^{Ca}$*atoDA*$^{Ec}$*adc*$^{Ca}$; Km$^R$ | This work |
| pS2313-MKs2 | Derivative of vector pSEVA2313 harboring the genes encoding a synthetic MK biosynthesis pathway; $P_{EM7}$→*thl*$^{Ca}$*pcaIJ*$^{Pp}$*adc*$^{Ca}$; Km$^R$ | This work |
| pS2313-MKs3 | Derivative of vector pSEVA2313 harboring the genes encoding a synthetic MK biosynthesis pathway; $P_{EM7}$→*phaA*$^{Cn}$*ctfAB*$^{Ca}$*adc*$^{Ca}$; Km$^R$ | This work |
| pSEVA438 | Standard expression vector carrying a 3-*m*Bz–inducible expression system; *oriV*(pBBR1); *xylS*, *Pm*; Sm$^R$/Sp$^R$ | Silva-Rocha et al.[63] |
| pS438-MKc | Derivative of vector pSEVA2313 harboring the genes encoding the canonical acetone biosynthesis pathway from *C. acetobutylicum*; XylS/*Pm*→*thl*$^{Ca}$*ctfAB*$^{Ca}$*adc*$^{Ca}$; Sm$^R$/Sp$^R$ | This work |
| pS438-MKs1 | Derivative of vector pSEVA438 harboring the genes encoding a synthetic MK biosynthesis pathway; XylS/*Pm*→*thl*$^{Ca}$*atoDA*$^{Ec}$*adc*$^{Ca}$; Sm$^R$/Sp$^R$ | This work |
| pSEVA4318 | Standard expression vector carrying a rhamnose-inducible expression system; *oriV* (pBBR1); *rhaR*, *rhaS*, $P_{rhaBAD}$; Sm$^R$/Sp$^R$ | Martínez-García et al.[64] Kozaeva et al.[44] |
| pS4318-MKc | Derivative of vector pSEVA4318 harboring the genes encoding the canonical acetone biosynthesis pathway from *C. acetobutylicum*; RhaRS/$P_{rhaBAD}$→*thl*$^{Ca}$*ctfAB*$^{C}$*adc*$^{Ca}$; Sm$^R$/Sp$^R$ | Kozaeva et al.[44] |
| pS4318-MKs1 | Derivative of vector pSEVA4318 harboring the genes encoding a synthetic MK biosynthesis pathway; RhaRS/$P_{rhaBAD}$→*thl*$^{Ca}$*atoDA*$^{Ec}$*adc*$^{Ca}$; Sm$^R$/Sp$^R$ | Kozaeva et al.[44] |
| pS4318-MKc-Acs | Derivative of vector pSEVA4318 harboring the genes encoding the canonical acetone biosynthesis pathway from *C. acetobutylicum* and an acetyl-CoA synthase gene (*acs*) from *Bacillus subtilis*; RhaRS/$P_{rhaBAD}$→*thl*$^{Ca}$*ctfAB*$^{Ca}$*adc*$^{Ca}$*acs*$^{Bs}$; Sm$^R$/Sp$^R$ | This work |
| pS4318-MKs1-Acs | Derivative of vector pSEVA4318 harboring the genes encoding a synthetic MK biosynthesis pathway and an acetyl-CoA synthase gene (*acs*) from *B. subtilis*; RhaRS/$P_{rhaBAD}$→*thl*$^{Ca}$*atoDA*$^{Ec}$*adc*$^{Ca}$*acs*$^{Bs}$; Sm$^R$/Sp$^R$ | This work |

[a]Antibiotic markers and abbreviations: *Km*, kanamycin; *Nal*, nalidixic acid; *Sm*, streptomycin; *Sp*, spectinomycin; *CoA*, coenzyme A; *MK*, methyl ketone; and 3-*m*Bz, 3-methylbenzoate. The source of relevant genes is indicated with a superscript as follows: *Ca*, *Clostridium acetobutylicum*; *Cn*, *Cupriavidus necator*; *Ec*, *Escherichia coli*; *Pp*, *Pseudomonas putida*; and *Bs*, *Bacillus subtilis*.

FtsZ assembly, whereas MinE acts as a negative regulator of MinCD. Minicells are formed when there is a limited abundance of MinC and MinD, whereupon FtsZ buildup promotes asymmetric cell division.[22] Unlike their parental counterparts, minicells do not contain chromosomal DNA and are unable to further divide; for this reason, they have historically been exploited as a model for studying protein synthesis.[23] In spite of their recognized potential as (mini)cell factories,[24] these chromosome-free bacterial vesicles have not been extensively exploited for bioproduction. Enhanced protein production, for instance, has been demonstrated in *Escherichia coli* minicells[25]—since plasmids are preferentially located at the poles of the parental bacterium,[26] their enrichment in minicells is facilitated *via* either active partitioning or random distribution. Moreover, cellular resources in the minicells (e.g., reducing power and energy equivalents) can be reasonably assumed to be allocated to bioproduction instead of housekeeping processes, e.g., genome maintenance and duplication. Among the microbial *chassis* implemented for metabolic engineering thus far, minicell applications have been exploited mostly for *E. coli* and *Bacillus subtilis*.[23] No attempts have been reported on producing these anucleated vesicles from *Pseudomonas putida*, an nonpathogenic soil bacterium extensively adopted for engineering applications.[27−30]

Building on the well-known solvent tolerance features of *P. putida*[31−34] and its ability of using a wide range of carbon sources,[35−39] we have engineered genome-reduced *P. putida* strains for biosynthesis of short-chain ($C_3$−$C_5$) (methyl) ketones from organic acids, with a focus on 2-pentanone production. The capacity of *Pseudomonas* species to produce long-chain MKs is illustrated by the model-guided engineering of *P. taiwanensis* VLB120,[40] which enabled the synthesis of $C_{11}$−$C_{17}$ MKs from sugars. In our study, the tolerance of *E. coli* and *P. putida* to products and substrates was compared, and production conditions were optimized for whole-cell 2-pentanone biosynthesis by using butanoate as the main substrate. Different synthetic pathway designs were likewise tested, analyzing the performance of constitutive and inducible expression systems across production conditions. Furthermore, we explored the potential of *P. putida* minicells for chemical production, adopting MKs as model compounds. Thus, we engineered *P. putida*-derived minicells to express selected pathway variants, demonstrating production of acetone, butanone and 2-pentanone from acetate, propanoate and butanoate, respectively. Programmable *P. putida* minicells had the ability to stably produce ketones over extended timeframes (up to 4 months)—a first case example of an "off-the-shelf" cell factory for MK biosynthesis. This strategy underscores the potential of integrating synthetic morphology with pathway


https://doi.org/10.1021/acssynbio.4c00700
ACS Synth. Biol. 2025, 14, 257−272

engineering as an alternative approach to sustainable ketone biosynthesis.

## RESULTS AND DISCUSSION

**Exploring the Potential of *P. putida* for Short-Chain Ketone Biosynthesis from Organic Acids.** A major challenge for efficient short-chain ketones production in engineered bacterial cell factories is the stress caused by the endogenously produced chemicals, which (similarly to other solvents)[41] could inhibit growth or even cause cell death.[42] While the biosynthesis of acetone (2-propanone, $C_3$) and butanone ($C_4$) by engineered microorganisms has been explored in the primary literature,[43−46] reports on biobased approaches for 2-pentanone ($C_5$) production are scarce. A study by Lan et al.[47] highlighted product toxicity as a key factor impairing 2-pentanone biosynthesis by engineered *E. coli* strains using glucose as a carbon source. The growth of *E. coli* JCL299, one of such modified strains,[47] was reported to be impaired by 50% in the presence of as little as 0.6 g $L^{-1}$ 2-pentanone, and bacterial growth was fully arrested when the concentration of the ketone reached 5 g $L^{-1}$. As *P. putida* is known to be a solvent-tolerant host, we explored its capacity for short-chain MK production, with 2-pentanone as a proxy of this family of compounds.

As a first step in testing the performance of *P. putida* as a production platform, we examined the effect of adding 2-pentanone to cultures of *P. putida* SEM1.3. Strain SEM1.3 is a refactored derivative of *P. putida* EM42,[48] a reduced-genome version of the platform strain KT2440 (Table 1).[49] The modifications introduced in *P. putida* SEM1.3 comprise (i) deletion of the *benABCD* gene cluster,[50] to abolish oxidation of 3-methylbenzoate (3-*m*Bz), allowing the use of this molecule as a gratuitous (i.e., nonmetabolizable) inducer of the XylS/*Pm* expression system without interfering with measurements of the optical density at 600 nm ($OD_{600}$) typically caused by brown-colored catechols and other products of aromatic compound metabolism[51] and (ii) elimination of the native *pha* gene cluster, *phaC1ZC2DFI*,[52] to avoid any potential metabolic cross-talk that could compete for acetyl-coenzyme A (CoA), key precursor for short-chain ketone biosynthesis *via* acetyl-CoA−dependent chain elongation. *P. putida* SEM1.3 was grown either in rich lysogeny broth (LB) or de Bont minimal (DBM) medium supplemented with 1% (w/v) glucose as the main carbon source and spiked with 2-pentanone at different concentrations (i.e., 1, 2.5, 5, 10, 25 and 50 g $L^{-1}$). Under all conditions tested, the impact of 2-pentanone on cell physiology was more evident when cells grew in a mineral medium than in a rich broth. Bacterial growth, assessed as the $OD_{600}$ values after 24 h, started to be affected at ketone concentrations above 5 g $L^{-1}$, but bacterial growth was still observed with up to 25 or 50 g $L^{-1}$ of 2-pentanone both in DBM medium or LB, respectively (Figure 1A). As an example, the final cell density was only reduced to ∼40% in LB medium spiked with 2-pentanone at 50 g $L^{-1}$. In general, *P. putida* SEM1.3 fared better under these conditions than *E. coli* JCL299, based on data reported in the literature.[47] These results illustrate the ability of *P. putida* to adapt to high solvent concentrations, a phenotype mediated by modifications in the surface of the outer membrane and other natural stress response mechanisms.[31] Next, we explored whether *P. putida* could utilize 2-pentanone as a carbon source by incubating strain SEM1.3 in DBM medium supplemented with 1 g $L^{-1}$ of 2-pentanone as the sole carbon substrate. The MK should not

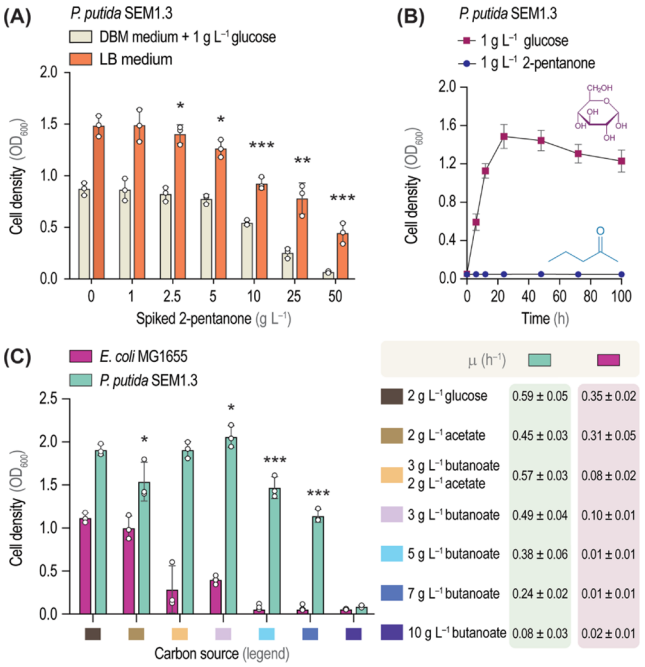


**Figure 1.** Exploring the tolerance of *P. putida* and *E. coli* to 2-pentanone and short-chain organic acids. (A) Physiological response of *P. putida* SEM1.3 to increasing concentrations of 2-pentanone, added to either de Bont minimal (DBM) medium or rich LB medium in microtiter plate cultures. Cell densities, estimated as the optical density at 600 nm ($OD_{600}$), were measured after 24 h of cultivation. (B) Growth profile of *P. putida* SEM1.3 cultivated on DBM medium containing either glucose or 2-pentanone as the sole carbon source. (C) Growth of *E. coli* MG1655 and *P. putida* SEM1.3 cultivated in DBM medium with different carbon sources (i.e., glucose, acetate, butanoate, or a combination of the two short-chain organic acids). Cell densities in these shaken-flask cultures, estimated as the $OD_{600}$, were measured after 24 h of cultivation; specific growth rates ($\mu$) were calculated during exponential growth. In all cases, mean values ± standard deviations were derived from independent biological triplicates. Significance levels of the cell density values when compared to control conditions [0 g $L^{-1}$ 2-pentanone for panel (A) and 2 g $L^{-1}$ glucose for panel (B)] are indicated as follows: *$P$-value <0.05, **$P$-value <0.01 and ***$P$-value <0.001.

mediate any toxicity at this relatively low concentration. Control experiments in DBM medium containing 1 g $L^{-1}$ glucose were run in parallel to benchmark growth patterns, and these cultures reached full saturation within 24 h (Figure 1B). No growth was detected when strain SEM1.3 was incubated with the ketone over 100 h (Figure 1B), indicating that *P. putida* is unable to utilize 2-pentanone as a substrate and underscoring its potential for short-chain MK bioproduction.

Another attractive metabolic feature of *P. putida*, i.e., efficient assimilation of organic acids as sole carbon source,[53] could be exploited for short-chain ketone biosynthesis. To examine this possibility, we evaluated butanoate as a substrate for 2-pentanone production. Butanoate, a $C_4$ carboxylic acid, can be processed by *Pseudomonas* through the canonical *β*-oxidation to yield acetyl-CoA.[54] Even though this carboxylate has not been actively investigated as a feedstock for bacterial fermentations, butanoate is a promising building-block that can be obtained from renewable resources[55] and it has been selected as a substrate for establishing high-cell-density *P. putida* cultures.[56] While these properties position butanoate as an interesting biorefinery substrate, osmotic


https://doi.org/10.1021/acssynbio.4c00700
ACS Synth. Biol. 2025, 14, 257−272

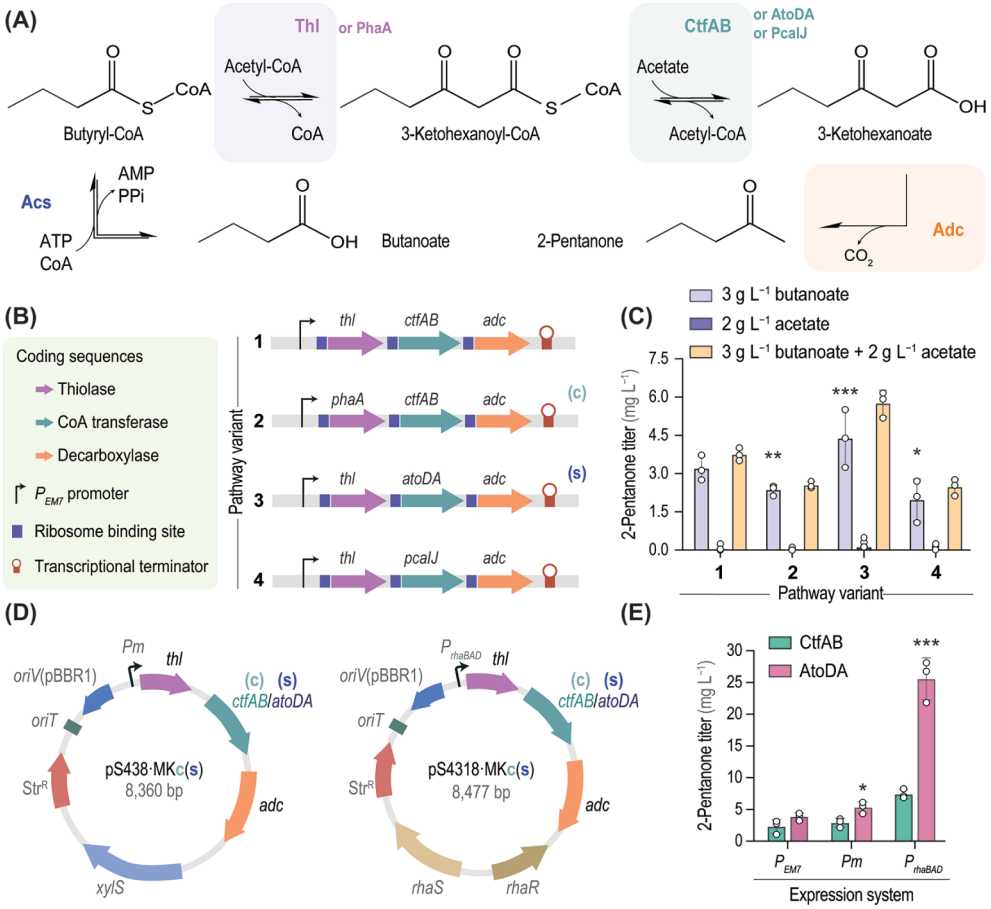


**Figure 2.** Pathway engineering and optimization for 2-pentanone biosynthesis from short-chain organic acids. (A) Biosynthetic pathway for 2-pentanone production from butanoate. Methyl ketone biosynthesis relies on the enzymes of the canonical acetone pathway from *C. acetobutylicum*, comprising Thl, thiolase (acetyl-CoA acetyltransferase, EC 2.3.1.9), CtfAB (acetoacetyl-CoA:acetate/butanoate CoA transferase, $\alpha$ and $\beta$ subunits, EC 2.8.3.9), and Adc (acetoacetate decarboxylase, EC 4.1.1.4). Enzyme variants are likewise indicated whenever relevant. Abbreviations: *CoA*, coenzyme A; *PPi*, inorganic pyrophosphate. (B) Synthetic operons constructed for 2-pentanone biosynthesis. The elements in this diagram are not drawn to scale. (C) Testing 2-pentanone biosynthesis from short-chain organic acids in engineered *P. putida*. Bacteria were individually transformed with plasmids pS2313·MK[c,s1-s3], carrying the synthetic operons shown in panel (B) under control of the constitutive $P_{EM7}$ promoter (Table 1), and incubated for 24 h in DBM medium with the different carbon source combinations indicated; 2-pentanone titers were quantified in culture supernatants by GC-FID. (D) Plasmids for inducible expression of the synthetic operons for 2-pentanone biosynthesis. The synthetic XylS/*Pm* and RhaRS/$P_{rhaBAD}$ expression systems are induced by addition of 3-methylbenzoate and rhamnose, respectively; both plasmids carry a streptomycin-resistance determinant ($Str^R$). (E) Exploring strain performance by growing *P. putida* SEM1.3 with the selected plasmids in DBM medium containing 3 g $L^{-1}$ butanoate for 24 h. 2-Pentanone titers in the culture supernatant were quantified by GC-FID; methyl ketone titers in strains carrying inducible expression systems are compared to the constitutive expression mediated by the $P_{EM7}$ promoter. Results shown in panel (C) and (E) correspond to mean values ± standard deviations from independent biological triplicates. Significance levels of 2-pentanone titers when compared to control conditions [pathway variant 1, spanning the canonical set of enzymes, for panel (C), and constitutive gene expression mediated by the $P_{EM7}$ promoter for panel (E)] are indicated as follows: *$P$-value <0.05, **$P$-value <0.01 and ***$P$-value <0.001.

shock and acid stress may result in toxicity issues even at relatively low concentrations.[57] To test this scenario, the tolerance of *P. putida* SEM1.3 and *E. coli* MG1655 (adopted as a model Gram-negative bacterium, extensively used as a host in diverse bioprocesses)[58] to increasing butanoate concentrations was evaluated and compared with widely used sugar and organic acid substrates (Figure 1C). Glucose or acetate were selected as the primary carbon feedstocks as representative examples of a glycolytic and a gluconeogenic substrate, respectively. *P. putida* SEM1.3 tolerated up to 7 g $L^{-1}$ butanoate with a reduction of ca. 45% in the final $OD_{600}$ values, while the growth of *E. coli* MG1655 was virtually abolished at any butanoate concentration above 3 g $L^{-1}$. Neither bacterial species could grow on DBM medium containing 10 g $L^{-1}$ butanoate, which marks the practical upper concentration to be used in production experiments. Interestingly, the cultures of *P. putida* SEM1.3 reached similar final $OD_{600}$ values when butanoate was either used as the sole carbon substrate or added at 3 g $L^{-1}$ in the presence of glucose or acetate. This observation indicates that butanoate is not a preferred carbon source in the presence of a cosubstrate.[59] The specific growth rate ($\mu$) was not affected by butanoate at concentrations <5 g $L^{-1}$ (Figure 1C), although we observed an increase (ca. 2 h) in the extension of the lag phase in these cultures. Building on these results, we adopted reduced-genome *P. putida* SEM1.3 as the host to explore the butanoate-dependent biosynthesis of 2-pentanone.

**Implementing and Optimizing Pathways for 2-Pentanone Biosynthesis from Organic Acids.** The canonical short-chain ketone biosynthesis route, key to the widely known fermentation process to produce acetone by *Clostridium acetobutylicum* ATCC 824 (the *Weizmann*


https://doi.org/10.1021/acssynbio.4c00700
ACS Synth. Biol. 2025, 14, 257−272

*organism*),[60] was adopted to explore MK biosynthesis by engineered *P. putida*. We hypothesized that this pathway could be coupled with CoA-dependent ketoacid chain elongation,[61,62] yielding butyryl-CoA ($C_4$) from acetyl-CoA ($C_2$) extender units. In this way, the core acetone biosynthesis pathway of *C. acetobutylicum* can be adjusted to produce a variety of short-chain ketones. For instance, biosynthesis of 2-pentanone ($C_5$) from butanoate involves the condensation of acetyl-CoA and butyryl-CoA (forming 3-ketohexanoyl-CoA) followed by ester hydrolysis and decarboxylation to yield the final product (Figure 2A). The sequence starts with the condensation of acetyl-CoA and butyryl-CoA mediated by a thiolase (Thl; acetyl-CoA acetyltransferase, EC 2.3.1.9). Next, CtfAB, an acetoacetyl-CoA:acetate/butanoate CoA transferase (EC 2.8.3.9) relocates a CoA moiety from 3-ketohexanoyl-CoA to acetate, forming 3-ketohexanoate. Finally, this molecule is reduced to 2-pentanone by an acetoacetate decarboxylase (Adc; EC 4.1.1.4), releasing $CO_2$ (Figure 2A). The theoretical ketone yield from organic acids through the canonical biosynthesis pathway shown in Figure 2A is $Y_{P/S}$ = 50% mol mol$^{-1}$.

Since all enzymes within the canonical biosynthesis route stem from a Gram-positive bacterium, we expanded the biochemical toolset for short-chain ketone production by harnessing activities from species phylogenetically closer to our host. The PhaA thiolase from *Cupriavidus necator* and the AtoDA and PcaIJ CoA transferases from *E. coli* MG1655 and *P. putida* KT2440, respectively, were considered for pathway design. The broad-host-range plasmids pS2313·MKc, MKs1, MKs2 and MKs3 (Table 1) were constructed with different combinations of genes encoding all pathway enzymes under transcriptional control of the constitutive $P_{EM7}$ promoter. A synthetic ribosome binding site[63] (RBS) was incorporated upstream each coding sequence (Figure 2B), and all plasmids were formatted according to the Standard European Vector Architecture (SEVA).[64] According to the plasmid nomenclature adopted in our study, constructs involving canonical pathway components are identified with a *c* letter (e.g., plasmid pS2313·MKc), whereas those bearing synthetic pathway variants are labeled with an *s* letter (e.g., plasmid pS2313·MKs1, where the canonical *ctfAB* genes are replaced by *atoDA* from *E. coli*, Table 1). The resulting plasmids (pS2313·MKc, MKs1, MKs2 and MKs3) were individually transformed into *P. putida* SEM1.3, and the ability of the engineered strains to produce 2-pentanone was tested in shaken-flask cultures using different carbon substrates. Cultures were grown for 24 h in DBM medium containing either 3 g L$^{-1}$ of butanoate, 2 g L$^{-1}$ of acetate or a combination of 3 g L$^{-1}$ of butanoate and 2 g L$^{-1}$ of acetate as the carbon substrate (s). By the end of the cultivation, 2-pentanone titers and the concentration of any residual carbon source(s) were determined in culture supernatants. Full consumption of the carbon substrate(s) was observed under all conditions. Acetate did not promote MK biosynthesis when used as a sole carbon substrate regardless of the biosynthetic pathway borne by strain SEM1.3 (Figure 2C). Constructs 1 (containing *thl*, *ctfAB* and *adc*) and 3 (spanning *thl*, *atoDA* and *adc*), in contrast, mediated the highest 2-pentanone titers (3.2 mg L$^{-1}$ and 4.5 mg L$^{-1}$, respectively) when butanoate was used as the feedstock. Cultures incubated in the presence of both acetate and butanoate grew to higher cell densities than those added with the individual organic acids, but 2-pentanone titers were not significantly different—suggesting that, under these conditions, butanoate was largely responsible for promoting ketone formation. The higher 2-pentanone titers attained by *P. putida* SEM13 carrying plasmid pS2313·MKs1 (construct 3) indicate that the AtoDA was the most efficient transferase variant. This feature is likely connected to the substrate affinity of AtoDA, which is 22-fold higher than that of CtfAB (*Km* for acetate = 53.1 mM and 1,200 mM, respectively).[65]

Considering the trade-offs between growth and production,[66−68] which compete for essential resources at the level of the acetyl-CoA node,[69] we evaluated whether regulated expression of the pathway genes could lead to higher ketone titers. The performance of strain SEM1.3 carrying constructs 1 and 3 under the control of different inducible expression systems was assayed for this purpose. A number of expression systems are available for engineering *P. putida*; including both native *Pseudomonas* regulatory elements (e.g., XylS/*Pm*, AlkS/$P_{alkB}$ and NahR/$P_{sal}$)[28] and heterologous modules (e.g., AraC/$P_{araB}$ and RhaRS/$P_{rhaBAD}$).[70] The XylS/*Pm* and RhaRS/$P_{rhaBAD}$ expression cassettes, inducible by 3-methylbenzoate (3-*m*Bz) and rhamnose, respectively, were selected owing to their reportedly tight inducer dependency[71] and the high levels of gene expression.[70] Hence, plasmids pS438·MKc and MKs1 (based on the XylS/*Pm* system) and pS4318·MKc and MKs1 (based on the RhaRS/$P_{rhaBAD}$ system) were constructed for regulated expression of the best-performing pathway designs (constructs 1 and 3, Table 1); the physical map of these plasmids is displayed in Figure 2D. These four new plasmids were individually introduced in *P. putida* SEM1.3, and the corresponding cultures were grown for 24 h in DBM medium with 3 g L$^{-1}$ of butanoate, assessing the 2-pentanone titers and residual carbon source concentrations by the end of the incubation (Figure 2E). The two inducers, 3-*m*Bz and rhamnose, were added at the onset of the cultivation (4 h) at 1 mM and 5 mM, respectively. In general, inducible expression of the different production pathways led to enhanced ketone titers when compared to constitutive gene expression. This positive effect was even more evident in cultures of *P. putida* SEM1.3 carrying construct 3 (which includes the AtoDA transferase), with a 2-pentanone titer of 25.3 ± 0.9 mg L$^{-1}$ paired to full substrate consumption.

We also investigated whether the activation of butanoate into butyryl-CoA could represent a metabolic bottleneck.[72] Previous experiments depended on the activity of the endogenous acetyl-CoA synthases (Acs) of *P. putida* (i.e., Acs-I and Acs-II),[73] necessary for generating the CoA-ester derivatives of the short-chain organic acid substrates. To investigate the potential of a heterologous acetyl-CoA synthetase in supporting butyryl-CoA formation, a well-characterized and highly efficient Acs from *Bacillus subtilis*[74] was integrated into pathway designs, resulting in plasmids pS4318·MK(c,s1)·Acs (Table 1). Testing 2-pentanone biosynthesis by *P. putida* SEM1.3 harboring these constructs, however, did not yield a substantial enhancement in product titers from butanoate (data not shown). We concluded that the activity of the endogenous Acs-I and Acs-II is probably sufficient for sustaining ketone biosynthesis, and the original pathway designs were retained for further experiments.

**Establishing Asymmetrical Cell Division in *P. putida* to Produce Minicells.** Based on the MK production capabilities of *P. putida*, along with its inherent tolerance to toxic chemicals, we hypothesized that minicells could be adopted as an alternative system for ketone biosynthesis. Minicells are nanosized (100−400 nm in diameter)


https://doi.org/10.1021/acssynbio.4c00700
ACS Synth. Biol. 2025, 14, 257−272

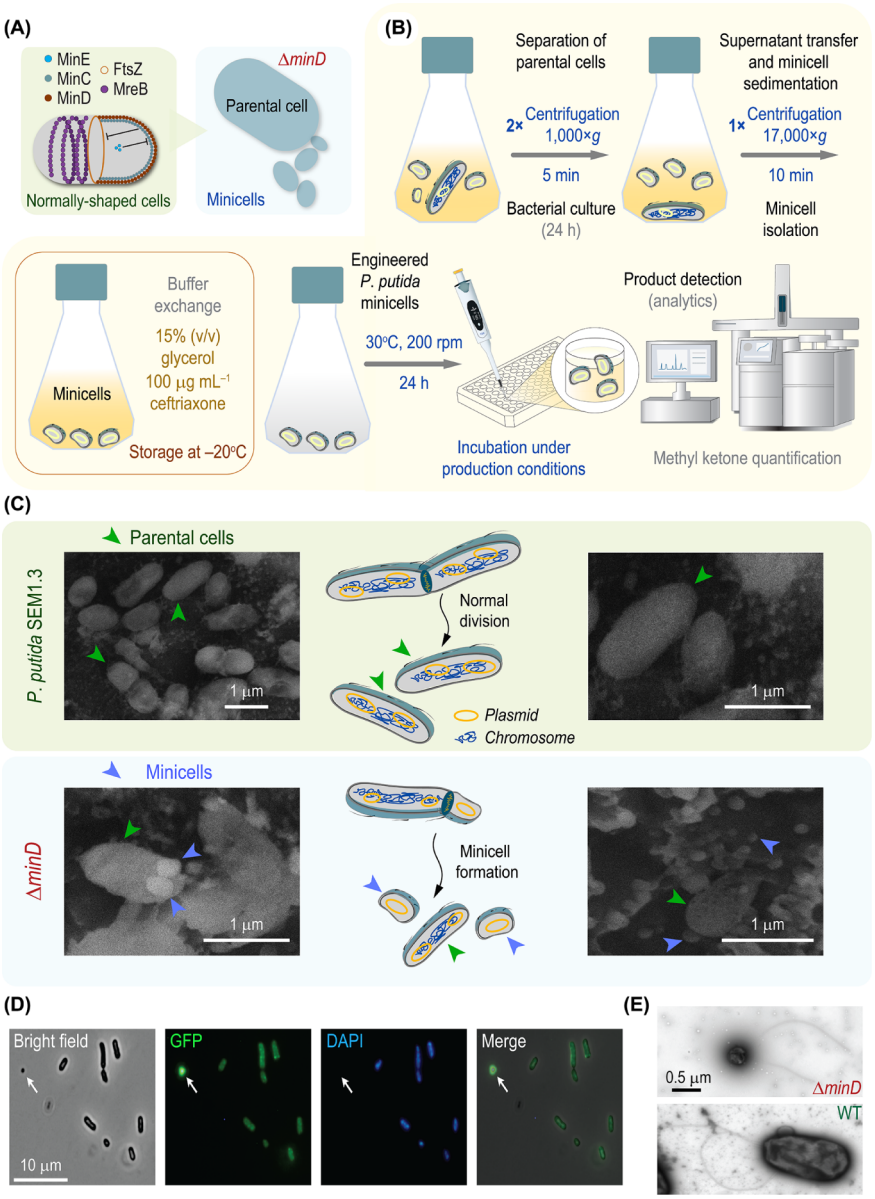


**Figure 3.** Production and characterization of *P. putida* minicells. (A) Key elements involved in cell division in Gram-negative bacteria. In normally shaped cells, the MinC−MinD−MinE system and the cell wall structural, actin-like MreB protein establish a dynamic equilibrium with FtsZ, the division protein, to ensure proper septation and segregation of daughter cells. Mutations in the Min components, e.g., the Z-ring positioning MinD protein, lead to minicell segregation. (B) Overview of the protocol for *P. putida* minicells production, purification, storage, and downstream applications. The minicell suspension can be either used immediately or stored at −20 °C or −70 °C upon buffer exchange. Whenever needed, the minicell preparation is incubated in microtiter plates under specific conditions to support product formation, and the metabolites of interest are detected by dedicated analytical methods. (C) Representative scanning electron cryomicroscopy (CryoSEM) images of strains *P. putida* SEM1.3 and its minicell-producing derivative. CryoSEM microscopy was performed on freeze-fractured samples from these cultures, imaged at 15 kV in an X-Max$^N$ 150 silicon drift detector (sensor-active area = 150 mm$^2$; Oxford Instruments NanoAnalysis) after a Pt-coating treatment. Parental cells and minicells are identified with green and blue arrowheads, respectively; the asymmetrical segregation of daughter cells leads to the formation of chromosome-free minicells that retain plasmid(s) from the parental bacterium. (D) Representative phase-contrast (bright field) and fluorescence merged images of GFP-fluorescence and DAPI staining of a Δ*minD* derivative of *P. putida* KT2440 carrying plasmid pS4413·*msfGFP*. The arrow marks the position of a bacterial minicell. (E) Representative thin-sectioned negative-stain micrographs (transmission electron microscopy, TEM) of the same strains (wild-type, WT, and a Δ*minD* mutant) shown in panel (D).

achromosomal bacteria, formed by abortive cell division in the mother cell poles.[23] Minicells cannot grow or duplicate, but they can support other vital cellular processes, e.g., ATP synthesis, replication and transcription of plasmid DNA and mRNA translation.[23] To the best of our knowledge, the production and engineering of *P. putida* minicells have not been reported thus far. We started by exploring the cell division mechanisms that could mediate abnormal bacterial segregation in this species. The normal process of cell division in *E. coli* and other rod-shaped bacteria, triggered by the formation of the *Z*-ring,[22] yields two equally sized daughter cells[75] (Figure 3A). In Gram-negative bacteria, the dynamics of the *Z*-ring assembly and location are regulated by the Min system.[76] MinD binds to the polar membrane to form a polymer, and the MinCD-complex inhibits FtsZ polymerization of by recruiting MinE—interfering with the membrane


https://doi.org/10.1021/acssynbio.4c00700
ACS Synth. Biol. 2025, 14, 257−272

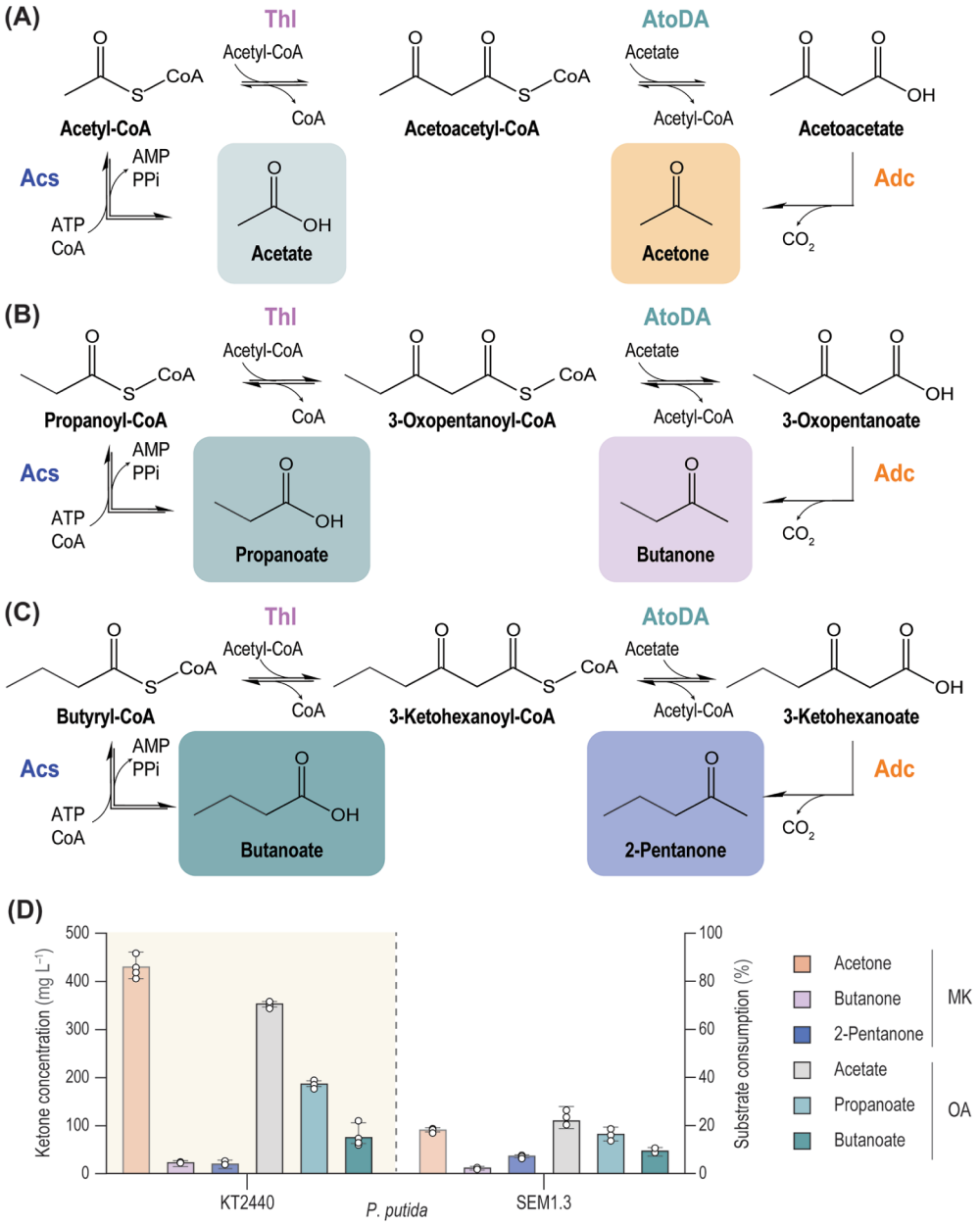


**Figure 4.** Exploring (methyl) ketone biosynthesis by *P. putida*. (A−C) Synthetic pathways tested for the bioconversion of different organic acids into short-chain (methyl) ketones by *P. putida* minicells. The selected pathways mediate the production of acetone from acetate ($C_2$) (A), butanone from propanoate ($C_3$) (B), and 2-pentanone from butanoate ($C_4$) (C). The theoretical yield for all (methyl) ketones shown in the diagram is $Y_{P/S}$ = 50% mol mol$^{-1}$. Abbreviations: *CoA*, coenzyme A; *PPi*, inorganic pyrophosphate. (D) Whole-cell biocatalysis experiments with *P. putida* SEM 1.3 and KT2440 were performed in the presence of acetate, propanoate or butanoate as the substrates for short-chain (methyl) ketone (MK) production. In all cases, *P. putida* strains were incubated with 50 mM of selected organic acid and 15% (v/v) glycerol. Both organic acid (OA) consumption and product (acetone, butanone and 2-pentanone) titers were determined after 24 h. Results correspond to mean values ± standard deviations from three independent biological triplicates.

assembly at an abnormal location.[24] Abnormal cell division ensues if the *Z*-ring is either formed at the cell pole or if the FtsZ division protein is overproduced, leading to minicell formation.[77] The Min system, thoroughly characterized in *E. coli* and *B. subtilis*, is widespread in bacterial species[19] including *Pseudomonas*. In strain KT2440, the *minCDE* genes form a cluster in the *PP_1732-PP_1734* locus, with the gene encoding the septum site-determining protein MinC as the last element in the sequence.[49] Previous experiments from our laboratory indicated that transcriptional interference on *minD* (*PP_1733*, encoding the ATPase component of the Min system) with a CRISPRi system tailored for *Pseudomonas* species[78] leads to the emergence of minicells.

The MinD-deficient *P. putida* strain was used to enrich the minicell population through a simple three-step protocol, based on sequential centrifugation (Figure 3B). This procedure yielded ca. 0.25 $g_{CDW}$ (cell dry weight) L$^{-1}$ minicells from a 1.5 $g_{CDW}$ L$^{-1}$ bacterial suspension. As an additional, optional step in the purification process, ceftriaxone, a broad-spectrum $\beta$-lactam, was added at 100 $\mu$g mL$^{-1}$ to the samples to eliminate any parental cells that might be present in the minicell suspension. At the last stage of the protocol, glycerol was


https://doi.org/10.1021/acssynbio.4c00700
ACS Synth. Biol. 2025, 14, 257−272

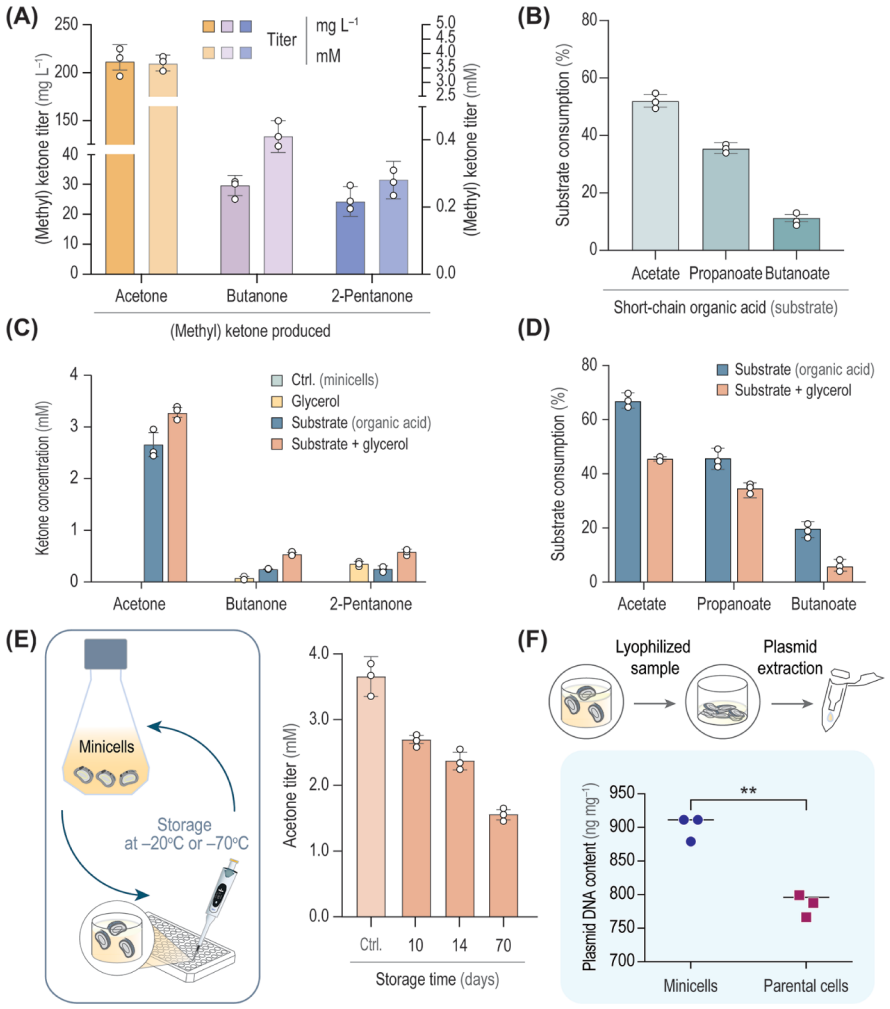


**Figure 5. Short-chain (methyl) ketone production by *P. putida* minicells.** (A) Bioconversion experiments performed using acetate, propanoate or butanoate as the substrate for short-chain (methyl) ketone biosynthesis by minicells. *P. putida* minicells were incubated in the presence of the selected organic acid (50 mM) and 15% (v/v) glycerol. Both product (acetone, butanone and 2-pentanone) titers (A) and substrate (acetate, propanoate and butanoate) consumption (B) were determined after 24 h. (C) The effect of glycerol on bioconversion of organic acids into (methyl) ketones was assessed after 18 h of incubation with 15% (v/v) glycerol and/or 50 mM of the corresponding organic acid substrate (acetate, propanoate or butanoate). *Ctrl.*, control. Substrate consumption by purified *P. putida* minicells under the same experimental conditions is indicated in panel (D). Acetate, propanoate or butanoate could not be detected in samples that were not supplemented with the corresponding substrates; therefore, these experiments are not included in the figure. (E) Acetone titers were used as a proxy for evaluating production phenotypes in *P. putida* minicells after storage at −70 °C in the presence of 15% (v/v) glycerol. Engineered minicells, prepared as indicated in Figure 3B, were tested for their ability to mediate the bioconversion of acetate (50 mM) into acetone. Acetone titers were compared to a control (Ctrl.) experiment conducted with freshly prepared *P. putida* minicells. Results shown in panels (A−E) represent mean values ± standard deviations from independent biological triplicates. (F) Plasmid DNA content in *P. putida* SEM1.3 and its minicell-producing derivative. Lyophilized samples (corresponding to 6.5 mg cell dry weight) were used to isolate plasmid DNA with a commercial kit; plasmid DNA content is expressed in ng DNA mg cell dry weight$^{-1}$. Results correspond to mean values ± standard deviations from three independent biological triplicates; significance levels are indicated with **$P$-value <0.01.

added to the minicell suspension at 15% (v/v) and the preparation can be kept at 4 °C or at −20 °C or −70 °C for extended storage.

To explore the minicell-forming phenotype, *P. putida* Δ*minD* and a derivative expressing the monomeric superfolder GFP (msfGFP) gene (Table 1) were grown in rich 2 × YT medium at 30 °C and harvested after 24 h. Aliquots of these cultures, along with the parental strain, were centrifuged, washed and prepared for scanning electron cryomicroscopy (cryoSEM), transmission electron microscopy (TEM) and fluorescence microscopy as indicated in *Methods*. CryoSEM was performed on freeze-fractured samples derived from these cultures, with imaging at 15 kV in an X-Max$^N$ 150 silicon drift detector. Image analysis identified the segregation of minicells at the poles of the Δ*minD* mutant (Figures 3C and S1A). The resulting anucleated vesicles were round-shaped, with a mean diameter in the 200−400 nm range, similar to the features reported for *E. coli* minicells.[79] In several instances, minicells were observed budding from normally rod-shaped parental bacteria (Figure S1B). Under these conditions, we could not observe any structure akin to outer membrane vesicles,[80] smaller than minicells and typically produced under stressful conditions.[81] Fluorescence microscopy revealed that the Δ*minD* strain carrying plasmid pS4413·*msfGFP* (Table 1) produced minicells loaded with the fluorescent protein but lacking chromosomal DNA, as indicated by 4′,6-diamidino-2-


https://doi.org/10.1021/acssynbio.4c00700
ACS Synth. Biol. 2025, 14, 257−272

phenylindole (DAPI) staining (Figure 3D). We also analyzed the phenotype of a Δ*minD* derivative of the wild-type strain KT2440 and observed that some minicells retained their flagella (Figure 3E), highlighting the value of adopting *P. putida* SEM1.3 Δ*minD* for biocatalysis. This strain lacks the flagellar machinery,[50] thereby conserving energy that can be redirected into bioproduction. Based on data from the literature,[82−84] a Δ*minD* bacterial cell typically undergoes 3−7 normal divisions before malfunctioning; hence, 12−28 minicells can be expected per mother cell. The features were exploited to test bioconversion of organic acids into value-added products as explained in the next section.

***P. putida* Minicells Mediate Bioconversion of Organic Acids into Short-Chain Ketones.** We tested the versatility of the short-chain MK biosynthesis pathway for testing the production of three different ketones by *P. putida* minicells. In particular, the enzymatic cascade composed by Thl and Adc from *C. acetobutylicum*, together with AtoDA from *E. coli*, could be leveraged for the synthesis of various (methyl) ketones by using different, readily available organic acids as feedstocks (e.g., acetate, propanoate and butanoate; Figure 4A−C). Sustainable methods for producing short-chain organic acids are attracting attention in biotechnology—a trend exemplified by the recent advances in $C_1$ assimilation processes for synthesizing building-blocks (e.g., acetate).[85−88] Acetate, in turn, has been exploited as a feedstock to drive efficient acetone production,[89] showing the potential of this $C_2$ carboxylate as a sustainable carbon source for biorefinery. The core biosynthesis pathway (Figure 2) could be adapted to produce acetone, butanone or 2-pentanone by feeding acetate ($C_2$, Figure 4A), propanoate ($C_3$, Figure 4B) or butanoate ($C_4$, Figure 4C) as the main substrate, respectively. In all cases, the theoretical (methyl) ketone yield on the organic acid substrate is $Y_{P/S}$ = 50% mol $mol^{-1}$. At the same time, we assessed whether a genome-reduced background influenced ketone production by comparing production formation in both *P. putida* KT2440 and SEM1.3 (Figure 4D). No significant differences were found for butanone and 2-pentanone, while increased substrate consumption and higher acetone titers were observed in experiments with strain KT2440 (Figure 4D).

Based on these observations, minicells derived from *P. putida* SEM1.3 Δ*minD* transformed with plasmid pS4318·MKs1 were used in bioconversion experiments by incubating the suspension with the three organic acids (i.e., acetate, propanoate and butanoate) at 50 mM. After 24 h, both ketone production (Figure 5A) and substrate consumption (Figure 5B) were assessed in the supernatants. Acetone titers reached 211 ± 18 mg $L^{-1}$, whereas the maximum butanone and 2-pentanone concentrations observed under the same conditions were 30 ± 3 mg $L^{-1}$ and 24 ± 6 mg $L^{-1}$, respectively (Figure 5A). The profile of short-chain MK production by minicells followed a trend similar to that of carboxylate utilization (Figure 5B). Under these conditions, between 11% and 52% of the carboxylates were consumed by the *P. putida* minicells, with a positive correlation between chain length and substrate consumption (Figure 5B).

**Evaluation of Operating Conditions for Short-Chain (Methyl) Ketone Biosynthesis by *P. putida* Minicells.** The minicell suspension, prepared as outlined in Figure 3B, was used to demonstrate the capacity of the anucleated bacterial vesicles for biotransformation of organic acids into methyl ketones. To investigate factors affecting catalytic activity, we conducted a series of experiments focusing on incubation conditions and metabolic stability of the minicells. In this sense, the final step of the isolation protocol involved adding glycerol at 15% (v/v) as a cryoprotectant for extended storage. Since glycerol can also serve as an energy and carbon source for *P. putida*,[90] we tested the potential contribution of this additive to product formation. Glycerol alone did not support acetone biosynthesis, and traces of butanone and 2-pentanone could be detected in the absence of organic acid substrates (Figure 5C). In all cases, we observed an additive effect of glycerol and the main substrate in promoting product formation. This observation was mirrored in the consumption of organic acids during the bioconversion experiments (Figure 5D). When glycerol was present in the incubation medium, substrate consumption decreased (with butanoate being particularly affected). These observations suggest a role for the polyol in supporting cellular processes, e.g., redox balancing,[91] beyond the expected cryoprotectant effect.

A relatively unexplored advantage of minicells for bioproduction is their catalytic stability, as they do not require resource investment or energy expenditure for cell division. We systematically assessed the stability of *P. putida* minicells after enrichment and purification (Figure 3B) by storing aliquots of the minicell suspension at −70 °C for extended periods (from 10 to 70 days). Periodically, individual minicell aliquots were retrieved from the freezer and used in 24-h acetone bioconversion experiments as described above. To establish a baseline, the ability of freshly purified minicells to convert acetate into acetone was analyzed immediately after purification (control condition, Figure 5E). Acetone titers showed relatively limited variability across all samples, with >50% of the acetone concentration retained in experiments performed with minicells stored for up to 70 days (Figure 5E). Interestingly, storing the minicells at −20 °C during the same period did not result in any significant decrease in product titers (data not shown). The parental cells had a much lower catalytic activity (<10%) upon 10 days of storage at −70 °C. Taken together, these results highlight the metabolic stability and robustness of *P. putida*-derived minicells and demonstrate their potential to produce toxic chemicals even after prolonged storage.

In connection with the stable production phenotypes observed in engineered minicells, we studied their plasmid DNA content. To this end, the pathway designed and optimized for 2-pentanone biosynthesis (borne by plasmid pS4318·MKs1, Figure 2) was transformed into *P. putida* SEM1.3 Δ*minD*. We reasoned that the asymmetrical, abortive division in this mutant would lead to the formation of minicells carrying plasmids, but no chromosomal DNA (Figure 3C). We compared the plasmid DNA content in minicells of *P. putida* SEM1.3 Δ*minD*, prepared as indicated in Figure 3B, and the parental strain. The plasmid DNA content in the minicells was 901 ± 19 ng $mg_{CDW}^{-1}$, which was ∼20% higher than that of the parental cells (Figure 5F). The stable maintenance of plasmids encoding the MK biosynthesis pathway helps to explain the observed production phenotypes. During bioconversion experiments using minicells, the acetone titers achieved corresponded to a $Y_{P/S}$ of ca. 28% of the theoretical maximum (Figure 5A), calculated based on acetate consumption (Figure 5B). The butanone and 2-pentanone levels reached in these experiments were higher than those attained by whole-cell biocatalysis (Figures 2E, 4D and 5A). This result is probably linked to increased stress tolerance, as previously


https://doi.org/10.1021/acssynbio.4c00700
ACS Synth. Biol. 2025, 14, 257−272

suggested for *E. coli* minicells.[92] Taken together, these observations indicate that the minicells retain the biosynthetic capabilities of their nucleated parental cells. Furthermore, these *P. putida* nanoreactors were able to produce all three target compounds even without further optimization steps (e.g., enhancing precursor channeling).[93]

## CONCLUSION

The biotechnological production of MKs and related molecules is a sustainable alternative to oil-derived chemical production. Here, *P. putida* was adapted and optimized for short-chain ketone production owing to its innate solvent tolerance and enhanced utilization of organic acids as a carbon source. Examining product and substrate toxicity in both *E. coli* and *P. putida* highlighted the value of *Pseudomonas* as a host for MK production. Next to this, whole-cell ketone production with butanoate as the main carbon source was explored by implementing several pathway designs and synthetic expression systems. This systematic analysis suggested an optimal combination of $Thl^{Ca}$, $AtoDA^{Ec}$ and $Adc^{Ca}$ elements, where the cognate genes are heterologously expressed under the transcriptional control of the rhamnose-inducible RhaRS/$P_{rhaBAD}$ system. This bioproduction setup is amenable to further optimization steps toward increasing product titers and yields, e.g., fed-batch cultivation[40] or cofeeding strategies.[94] Given the known promiscuity of the enzymes in this pathway, byproduct formation should be carefully monitored during production process optimization, particularly at high MK titers.

Engineered chromosome-free *P. putida* minicells were adopted to explore alternative approaches for short-chain MK bioproduction. *E. coli* minicells have been exploited for sugar-dependent production of $C_6$−$C_{10}$ alcohols and esters,[92] isobutanol and lycopene[95]—leading to titers that often exceeded those obtained by whole-cell biocatalysis. In our study, all three MKs of interest ($C_3$−$C_5$) could be produced by the engineered *P. putida* minicells through bioconversion of $C_{n-1}$ organic acids. The catalytic lifespan of minicells generally surpassed that of their parental cells, providing a distinct advantage for bioproduction. Yet, several aspects of the minicell bioconversion process can be subjected to optimization. For example, ceftriaxone, while not essential for MK production, could potentially increase costs and have potential environmental impacts. In this proof-of-concept study, the antibiotic was used to limit parental cell growth, ensuring the purity of the minicell preparation and the accuracy of characterization experiments. Additionally, alternative methods (e.g., CRISPR interference)[96−98] could be explored to induce minicell formation and ease strain construction, while potentially eliminating the need for purification steps. Together with these optimization steps, a systematic analysis of resource allocation (e.g., ATP and reducing equivalents) would illuminate further engineering steps to maximize minicell-based bioproduction of chemicals and proteins.

Finally, the results in this study not only underscore an alternative bioproduction strategy for chemical commodities,[99] but they also suggest further applications for biosensing[100] and the delivery of other cargoes (e.g., proteins). In this sense, bacterial minicells can be programmed to target cancer cells;[101] since some short-chain ketones have been shown to impair carcinogenesis,[7] this feature could be leveraged for designing advanced therapies.

## METHODS

**Bacterial Strains, Plasmids, and Culture Conditions.** The bacterial strains and plasmids used in this study are presented in Table 1; DNA oligonucleotides and gene fragments are listed in Tables S1 and S2, respectively. *E. coli* cultures were incubated at 37 °C and *P. putida* cultures were grown at 30 °C either in microtiter plate cultures or shaken-flask cultures as specified in the figure legends. Lysogeny broth (LB)[102] was composed of 10 g $L^{-1}$ tryptone, 5 g $L^{-1}$ yeast extract and 10 g $L^{-1}$ NaCl; solid culture media additionally contained 15 g $L^{-1}$ agar. LB was employed for cloning procedures and genome engineering manipulations. Rich 2 × YT medium (16 g $L^{-1}$ tryptone, 10 g $L^{-1}$ yeast extract and 5 g $L^{-1}$ NaCl) was used to produce *P. putida* minicells. In other physiology experiments and unless otherwise specified, de Bont minimal (DBM) medium[103] was used; the medium composition is detailed in Table S3. Growth kinetics and related parameters during physiological characterization of bacterial strains were derived from measurements of the optical density at 600 nm ($OD_{600}$) with light path correction in a Synergy MX microtiter plate reader (BioTek Instruments Inc., Winooski, VT, USA). For whole-cell 2-pentanone production by engineered *P. putida* strains, cultures were initiated from a saturated inoculum, previously grown for 18 h in DBM medium with the same carbon substrate(s) and additives to be used in the main experiment, at a starting $OD_{600}$ of 0.05. Cells were incubated for 24 h at 30 °C with constant rotary agitation at 200 rpm (MaxQ 8000 shaker incubator; Thermo Fisher Scientific Co., Waltham, MA, USA) in 10 mL of DBM medium placed in a 50 mL Erlenmeyer flask with the corresponding antibiotics and chemical inducers needed for induction of the pathway genes,[104−108] as indicated in the figure legends. Whenever needed, streptomycin (Sm) and kanamycin (Km) were added at 100 $\mu$g $mL^{-1}$ and 50 $\mu$g $mL^{-1}$, respectively. The $OD_{600}$ values in shaken-flask cultures were periodically recorded in a GENESYS 20 spectrophotometer (Thermo Fisher Scientific Co.) to estimate bacterial growth; in all cases, $OD_{600}$ data were processed and analyzed with the QurvE software.[109] The cultures were harvested after 24 h and the flasks were kept at 4 °C for 1 h, whereupon the bacterial biomass was recovered by centrifugation at 5,000 × *g* for 15 min and 4 °C. The concentration of substrates and products in the resulting supernatants was analyzed by HPLC or GC-FID as indicated below.

**General Cloning Procedures and Construction of Plasmids and Engineered Strains.** Unless stated otherwise, uracil-excision (*USER*) cloning[110] was used for plasmid construction; the AMUSER tool[111] was employed for designing the necessary oligonucleotides. Phusion *U* high-fidelity DNA polymerase (Thermo Fisher Scientific Co.) was used according to the manufacturer's specifications in DNA amplifications intended for *USER* cloning. For colony PCR amplifications, the commercial *OneTaq* master mix (New England BioLabs, Ipswich, MA, USA) was used according to the supplier's instructions. Chemically competent *E. coli* DH5$\alpha$ $\lambda$*pir* (Table 1) was prepared using the commercially available Mix and Go transformation kit (Zymo Research International, Irvin, CA, USA) according to the manufacturer's indications. These cells were used for plasmid maintenance and other routinary cloning procedures according to well-established molecular biology protocols.[112−116] The sequence of all used plasmids and bacterial strains was verified by Mix2Seq


https://doi.org/10.1021/acssynbio.4c00700
ACS Synth. Biol. 2025, 14, 257−272

sequencing (Eurofins Genomics, Ebersberg, Germany). Plasmids were delivered into *P. putida* by electroporating around 300 ng of plasmid DNA into 80 $\mu$L of a freshly prepared suspension of electrocompetent cells. *P. putida* was rendered electrocompetent by washing four times (by centrifugation and resuspension) the biomass from 4 mL of an overnight culture in LB medium with a 300 mM sucrose solution.[35] Electroporations were performed with a Gene Pulser XCell (Bio-Rad Laboratories Inc., Hercules, CA, USA) set to 2.5 kV, 25 $\mu$F capacitance and 200 Ω resistance in a 2 mm gap cuvette. Gene deletions were performed by allelic exchange as described previously.[117−119]

**Preparation and Storage of *P. putida* Minicells.** Precultures for minicell production were grown for 18 h in LB medium containing either 50 $\mu$g mL$^{-1}$ Km or 100 $\mu$g mL$^{-1}$ Sm (for plasmid-carrying cells), used to inoculate 2 × YT medium likewise added with Km or Sm as needed at an initial $OD_{600}$ = 0.05. These 100 mL cultures (placed in 500 mL baffled Erlenmeyer flasks) were grown at 30 °C with rotary agitation of 150 rpm (Innova 42 Incubator Shaker; New Brunswick Scientific Co., Edison, NJ, USA). After 24 h of incubation, the cultures were harvested for minicell purification following the procedure indicated in Figure 3B. After purification, the resulting minicell samples in 50 mM phosphate buffer saline (pH = 7.0) were mixed with glycerol at 15% (v/v) and ceftriaxone at 100 $\mu$g mL$^{-1}$ (to prevent bacterial contamination and eliminate any parental cell in the final minicell suspension) toward storing the samples at −20 °C or −70 °C.

**2-Pentanone Toxicity Tests.** The tolerance of *P. putida* strains to 2-pentanone was assessed in two experimental setups, in either 50 mL Falcon tubes or in microtiter plate cultures, with samples taken every 1 h or at 15 min intervals, respectively, over 72 h. Experiments were performed in biological triplicates using either LB medium or DBM medium containing 1% (w/v) glucose as the main carbon source. Microtiter plates were covered with a Breath-Easy sealing membrane (Sigma-Aldrich Co., St. Louis, MO, USA) and $OD_{600}$ readings were recorded automatically under continuous shaking in an Elx808 absorbance microplate reader (BioTek Instruments Inc.).

**Detection and Quantification of MKs and Organic Acids by HPLC and GC-FID.** Culture samples (10 mL) were cooled down in an ice bath and transferred into prechilled, 50 mL conical tubes. Culture supernatants, obtained as indicated above, were extracted with hexane (200 $\mu$L) and the organic phase was separated by centrifugation for 10 min at 4,500 × *g* at 4 °C. The organic phase samples were analyzed by gas chromatography (GC) with flame-ionization detection (FID) in a Trace 1300 gas chromatograph (Thermo Fisher Scientific Co.). The separation of products was carried out using an Agilent HP-INNOWax capillary column; the results were analyzed using the Chromeleon chromatography data system software version 7.1.3 (Thermo Fisher Scientific Co.). Quantification of products was performed by generating a standard calibration curve from the integrated area of spiked samples and calculating the corresponding concentration(s) in experimental samples by the integrated area of their respective peaks. For minicell experiments, the concentrations of acetone, butanone and 2-pentanone as well as that of acetate, propanoate and butanoate were measured by HPLC. A Dionex UltiMate 3000 HPLC system equipped with an Aminex HPX-87X ion exclusion (300 × 7.8 mm) column (Bio-Rad Laboratories Inc.) coupled to a Shodex RI-150 refractive index was used in these measurements. The column was maintained at 30 °C, the mobile phase consisted of 5 mM $H_2SO_4$ in Milli-Q water at a flow rate of 0.6 mL min$^{-1}$, with a run length of 45 min. HPLC data were processed using the Chromeleon chromatography data system software version 7.1.3 (Thermo Fisher Scientific Co.). The acetone concentration was monitored by refractive index detection, and compound concentrations were calculated from the corresponding peak areas using a calibration curve prepared with authentic standards of acetone, butanone, 2-pentanone, sodium acetate, sodium propanoate and sodium butanoate (in all cases, > 99% HPLC standards were used; Sigma-Aldrich Co.).

**Synthesis of Short-Chain MKs in Bioconversion Experiments Using *P. putida*Minicells.** Production of short-chain ketones was assayed in minicells using different carboxylates as substrates. Sodium acetate, sodium propanoate and sodium butanoate were selected to evaluate the production of acetone, butanone and 2-pentanone, respectively. The selected carboxylate was added to 235 $\mu$L of the minicell suspension (ca. 0.5 $g_{CDW}$ L$^{-1}$) at a concentration of 50 mM (final volume = 240 $\mu$L); the mixtures were incubated at 30 °C with rotary agitation at 180 rpm (Innova 42 Incubator Shaker) for 24 h. The formation of the corresponding short-chain ketones was analyzed by HPLC and calculated as described above; equivalent assays were performed in parallel to study the consumption of the selected carboxylates.

**Scanning Electron Cryomicroscopy (CryoSEM), Transmission Electron Microscopy (TEM), and Fluorescence Microscopy for Minicell Visualization and Characterization.** CryoSEM was done to observe the morphology of individual cells in bacterial cultures of *P. putida* SEM1.3 and its minicell-producing derivative. Cells were grown in 2 × YT medium at 30 °C with agitation at 150 rpm and harvested after 24 h, the $OD_{600}$ of every sample was normalized to 1, and purification of minicells was done as indicated in Figure 3B. The protocol consisted of the following steps: (i) the parental *P. putida* cells were sedimented by centrifugation at low speed (5 min at 1,000 × *g* and 4 °C, two times), (ii) the supernatant was carefully transferred into a new Falcon tube and centrifuged at 17,000 × *g* for 10 min to recover *P. putida* minicells and (iii) the resulting minicell pellet was resuspended in 5 mL of the buffer of choice (typically, 50 mM phosphate buffered saline, pH = 7.0). For quality control and phenotype validation, microscopy analysis was performed using CryoSEM of a freeze-fractured sample, coated with gold, and imaged at 15 kV in an X-Max$^N$ 150 silicon drift detector (sensor-active area = 150 mm$^2$; Oxford Instruments NanoAnalysis, Abingdon, United Kingdom). The bead was mounted for CryoSEM analysis on a sample holder attached to a transfer rod, rapidly frozen by plunging into slushed liquid nitrogen ($N_2$) at −210 °C and transferred to the preparation chamber at −180 °C (PP2000 CryoTransfer System; Quorum Technologies, Laughton, East Sussex, United Kingdom). Frozen samples were cleaved with a cold knife (facilitating an exposed surface in the fractured sample), sublimated at −80 °C for 15 min and coated with Pt at a current of 4.5 mA for 30 s. The samples were transferred under vacuum to the SEM stage in a field-emission scanning electron microscope (Quanta 200 FEG; FEI Co., Hillsboro, OR, USA) and imaged at 10 kV using an Everhart−Thornley detector. The pore size distribution was analyzed using the ImageJ software (version


https://doi.org/10.1021/acssynbio.4c00700
ACS Synth. Biol. 2025, 14, 257−272

1.50b; National Institutes of Health, Bethesda, MD, USA). DAPI staining of *P. putida* followed established protocols.[120] TEM and fluorescence microscopy of minicell suspensions were performed as described by MacDiarmid et al.[121] and Martínez-García et al.,[122] respectively.

**Data and Statistical Analysis.** All the experiments reported were independently repeated at least in three independent biological replicates (as indicated in the corresponding figure legend), and the mean value of the corresponding parameter ± standard deviation is presented. When relevant, the level of significance of differences when comparing results was evaluated by ANOVA (Bartlett's test) with $\alpha = 0.001$, 0.01 or 0.05, as indicated in the figure legends. Data analysis was performed with MS Excel (Microsoft Corp., Redmond, WA, USA) and Prism 8 (GraphPad Software Inc., San Diego, CA, USA) unless differently specified.

## ■ ASSOCIATED CONTENT

### Supporting Information

The Supporting Information is available free of charge at https://pubs.acs.org/doi/10.1021/acssynbio.4c00700.

Cryo-scanning electron microscopy (SEM) imaging of bacterial cells (Figure S1); oligonucleotides used in this work (Table S1); gene fragments used in this work (Table S2) composition of de Bont minimal medium (Table S3) (PDF)

## ■ AUTHOR INFORMATION


### Corresponding Author

**Pablo Iván Nikel** − *The Novo Nordisk Foundation Center for Biosustainability, Technical University of Denmark, Kongens Lyngby 2800, Denmark;* orcid.org/0000-0002-9313-7481; Email: pabnik@biosustain.dtu.dk

### Authors

**Ekaterina Kozaeva** − *The Novo Nordisk Foundation Center for Biosustainability, Technical University of Denmark, Kongens Lyngby 2800, Denmark;* Present Address: Department of Bioengineering, Stanford University, Stanford, CA, USA

**Manuel Nieto-Domínguez** − *The Novo Nordisk Foundation Center for Biosustainability, Technical University of Denmark, Kongens Lyngby 2800, Denmark*

**Kent Kang Yong Tang** − *The Novo Nordisk Foundation Center for Biosustainability, Technical University of Denmark, Kongens Lyngby 2800, Denmark;* Present Address: Novo Nordisk A/S, Hovedstaden, Denmark

**Maximilian Stammnitz** − *Centre for Genomic Regulation, Barcelona 08003, Spain*

Complete contact information is available at: https://pubs.acs.org/10.1021/acssynbio.4c00700


### Author Contributions

[§]E.K. and M.N-.D. contributed equally to this work and should be considered joint first authors. E.K.: conceptualization, investigation, formal analysis, validation, supervision, methodology, visualization, and writing—original draft; M.N.D.: investigation, formal analysis, validation, methodology, and visualization; K.K.Y.T.: investigation and methodology; M.S.: investigation, formal analysis, and methodology; P.I.N.: conceptualization, resources, supervision, methodology, project administration, funding acquisition, writing—review and editing, visualization, and data curation.

### Notes

The authors declare no competing financial interest.

## ■ ACKNOWLEDGMENTS

We are indebted to the Microscopy Team, especially the characterization specialist Marie Karen Tracy Hong Lin at DTU NanoLab (National Centre for Nano Fabrication and Characterization, Technical University of Denmark), for their help with the processing of the samples and visualization by cryo-SEM. E.K. was the recipient of a fellowship from the Novo Nordisk Foundation as part of the Copenhagen Bioscience Ph.D. Programme (Cohort 2017), supported through grant NNF17CC0026768. M.N.D. acknowledges the support received from the European Union's *Horizon2020* Research and innovation program under the Marie Sklodowska-Curie grant agreement No. 713683 (*COFUNDfellowsDTU*) and from the VELUX Foundation under the Villum Experiment program (grant No. 40979). The financial support from the Novo Nordisk Foundation (grants NNF18OC0034818, NNF20CC0035580, and NNF21OC0067996) to P.I.N. is also gratefully acknowledged.

## ■ REFERENCES


(1) Goh, E. B.; Baidoo, E. E.; Keasling, J. D.; Beller, H. R. Engineering of bacterial methyl ketone synthesis for biofuels. *Appl. Environ. Microbiol.* **2012**, *78*, 70−80.

(2) Grütering, C.; Honecker, C.; Hofmeister, M.; Neumann, M.; Raße-Lange, L.; Du, M.; Lehrheuer, B.; von Campenhausen, M.; Schuster, F.; Surger, M.; et al. Methyl ketones: a comprehensive study of a novel biofuel. *Sust. Energy Fuels* **2024**, *8*, 2059−2072.

(3) Park, J.; Rodríguez-Moyá, M.; Li, M.; Pichersky, E.; San, K. Y.; Gonzalez, R. Synthesis of methyl ketones by metabolically engineered *Escherichia coli*. *J. Ind. Microbiol. Biotechnol.* **2012**, *39*, 1703−1712.

(4) Scognamiglio, J.; Letizia, C. S.; Api, A. M. Fragrance material review on cyclohexyl methyl pentanone. *Food Chem. Toxicol.* **2013**, *62*, S138−S143.

(5) Dong, J.; Chen, Y.; Benites, V. T.; Baidoo, E. E. K.; Petzold, C. J.; Beller, H. R.; Eudes, A.; Scheller, H. V.; Adams, P. D.; Mukhopadhyay, A.; et al. Methyl ketone production by *Pseudomonas putida* is enhanced by plant-derived amino acids. *Biotechnol. Bioeng.* **2019**, *116*, 1909−1922.

(6) He, Z. T.; Hartwig, J. F. Enantioselective α-functionalizations of ketones *via* allylic substitution of silyl enol ethers. *Nat. Chem.* **2019**, *11*, 177−183.

(7) Pettersson, J.; Karlsson, P. C.; Göransson, U.; Rafter, J. J.; Bohlin, L. The flavouring phytochemical 2-pentanone reduces prostaglandin production and COX-2 expression in colon cancer cells. *Biol. Pharm. Bull.* **2008**, *31*, 534−537.

(8) Calero, P.; Nikel, P. I. Chasing bacterial *chassis* for metabolic engineering: a perspective review from classical to non-traditional microorganisms. *Microb. Biotechnol.* **2019**, *12*, 98−124.

(9) Cho, J. S.; Kim, G. B.; Eun, H.; Moon, C. W.; Lee, S. Y. Designing microbial cell factories for the production of chemicals. *JACS Au.* **2022**, *2*, 1781−1799.

(10) Gurdo, N.; Volke, D. C.; Nikel, P. I. Merging automation and fundamental discovery into the design−build−test−learn cycle of nontraditional microbes. *Trends Biotechnol.* **2022**, *40*, 1148−1159.

(11) Gurdo, N.; Volke, D. C.; McCloskey, D.; Nikel, P. I. Automating the design-build-test-learn cycle towards next-generation bacterial cell factories. *New Biotechnol.* **2023**, *74*, 1−15.

(12) Ezeji, T.; Milne, C.; Price, N. D.; Blaschek, H. P. Achievements and perspectives to overcome the poor solvent resistance in acetone and butanol-producing microorganisms. *Appl. Microbiol. Biotechnol.* **2010**, *85*, 1697−1712.

(13) Sarria, S.; Kruyer, N. S.; Peralta-Yahya, P. Microbial synthesis of medium-chain chemicals from renewables. *Nat. Biotechnol.* **2017**, *35*, 1158−1166.
(14) Boy, C.; Lesage, J.; Alfenore, S.; Guillouet, S. E.; Gorret, N. Co-expression of an isopropanol synthetic operon and eGFP to monitor the robustness of *Cupriavidus necator* during isopropanol production. *Enzyme Microb. Technol.* **2022**, *161*, 110114.
(15) Cornillot, E.; Nair, R. V.; Papoutsakis, E. T.; Soucaille, P. The genes for butanol and acetone formation in *Clostridium acetobutylicum* ATCC 824 reside on a large plasmid whose loss leads to degeneration of the strain. *J. Bacteriol.* **1997**, *179*, 5442−5447.
(16) Fernández-Cabezón, L.; Cros, A.; Nikel, P. I. Evolutionary approaches for engineering industrially-relevant phenotypes in bacterial cell factories. *Biotechnol. J.* **2019**, *14*, 1800439.
(17) Fan, C.; Davison, P. A.; Habgood, R.; Zeng, H.; Decker, C. M.; Gesell Salazar, M.; Lueangwattanapong, K.; Townley, H. E.; Yang, A.; Thompson, I. P.; et al. Chromosome-free bacterial cells are safe and programmable platforms for synthetic biology. *Proc. Natl. Acad. Sci. U.S.A.* **2020**, *117*, 6752−6761.
(18) Rampley, C. P. N.; Davison, P. A.; Qian, P.; Preston, G. M.; Hunter, C. N.; Thompson, I. P.; Wu, L. J.; Huang, W. E. Development of *SimCells* as a novel *chassis* for functional biosensors. *Sci. Rep.* **2017**, *7*, 7261.
(19) Frazer, A. C.; Curtiss, R. Production, properties and utility of bacterial minicells. *Curr. Top. Microbiol. Immunol.* **1975**, *69*, 1−84.
(20) Rothfield, L.; Taghbalout, A.; Shih, Y. L. Spatial control of bacterial division-site placement. *Nat. Rev. Microbiol.* **2005**, *3*, 959−968.
(21) Rowlett, V. W.; Margolin, W. The Min system and other nucleoid-independent regulators of *Z* ring positioning. *Front. Microbiol.* **2015**, *6*, 478.
(22) Harry, E. J. Bacterial cell division: regulating *Z*-ring formation. *Mol. Microbiol.* **2001**, *40*, 795−803.
(23) Farley, M. M.; Hu, B.; Margolin, W.; Liu, J. Minicells, back in fashion. *J. Bacteriol.* **2016**, *198*, 1186−1195.
(24) Volke, D. C.; Nikel, P. I. Getting bacteria in shape: synthetic morphology approaches for the design of efficient microbial cell factories. *Adv. Biosyst.* **2018**, *2*, 1800111.
(25) Yu, H.; Khokhlatchev, A. V.; Chew, C.; Illendula, A.; Conaway, M.; Dryden, K.; Maeda, D. L. N. F.; Rajasekaran, V.; Kester, M.; Zeichner, S. L. Minicells from highly genome reduced *Escherichia coli*: cytoplasmic and surface expression of recombinant proteins and incorporation in the minicells. *ACS Synth. Biol.* **2021**, *10*, 2465−2477.
(26) Million-Weaver, S.; Camps, M. Mechanisms of plasmid segregation: have multicopy plasmids been overlooked? *Plasmid* **2014**, *75*, 27−36.
(27) Nikel, P. I.; de Lorenzo, V. *Pseudomonas putida* as a functional *chassis* for industrial biocatalysis: from native biochemistry to *trans*-metabolism. *Metab. Eng.* **2018**, *50*, 142−155.
(28) Martínez-García, E.; de Lorenzo, V. *Pseudomonas putida* as a synthetic biology *chassis* and a metabolic engineering platform. *Curr. Opin. Biotechnol.* **2024**, *85*, 103025.
(29) Weimer, A.; Kohlstedt, M.; Volke, D. C.; Nikel, P. I.; Wittmann, C. Industrial biotechnology of *Pseudomonas putida*: advances and prospects. *Appl. Microbiol. Biotechnol.* **2020**, *104*, 7745−7766.
(30) de Lorenzo, V.; Pérez-Pantoja, D.; Nikel, P. I. *Pseudomonas putida* KT2440: the long journey of a soil-dweller to become a synthetic biology *chassis*. *J. Bacteriol.* **2024**, *206*, e00136−24.
(31) Bitzenhofer, N. L.; Kruse, L.; Thies, S.; Wynands, B.; Lechtenberg, T.; Rönitz, J.; Kozaeva, E.; Wirth, N. T.; Eberlein, C.; Jaeger, K. E.; et al. Towards robust *Pseudomonas* cell factories to harbour novel biosynthetic pathways. *Essays Biochem.* **2021**, *65*, 319−336.
(32) Nikel, P. I.; Martínez-García, E.; de Lorenzo, V. Biotechnological domestication of pseudomonads using synthetic biology. *Nat. Rev. Microbiol.* **2014**, *12*, 368−379.
(33) Blank, L. M.; Ionidis, G.; Ebert, B. E.; Bühler, B.; Schmid, A. Metabolic response of *Pseudomonas putida* during redox biocatalysis in the presence of a second octanol phase. *FEBS J.* **2008**, *275*, 5173−5190.
(34) Domínguez-Cuevas, P.; González-Pastor, J. E.; Marqués, S.; Ramos, J. L.; de Lorenzo, V. Transcriptional tradeoff between metabolic and stress-response programs in *Pseudomonas putida* KT2440 cells exposed to toluene. *J. Biol. Chem* **2006**, *281*, 11981−11991.
(35) Martínez-García, E.; Aparicio, T.; de Lorenzo, V.; Nikel, P. I. New transposon tools tailored for metabolic engineering of Gram-negative microbial cell factories. *Front. Bioeng. Biotechnol.* **2014**, *2*, 46.
(36) Nikel, P. I.; Silva-Rocha, R.; Benedetti, I.; de Lorenzo, V. The private life of environmental bacteria: pollutant biodegradation at the single cell level. *Environ. Microbiol.* **2014**, *16*, 628−642.
(37) Nikel, P. I.; Chavarría, M.; Fuhrer, T.; Sauer, U.; de Lorenzo, V. *Pseudomonas putida* KT2440 strain metabolizes glucose through a cycle formed by enzymes of the Entner-Doudoroff, Embden-Meyerhof-Parnas, and pentose phosphate pathways. *J. Biol. Chem.* **2015**, *290*, 25920−25932.
(38) Nikel, P. I.; Romero-Campero, F. J.; Zeidman, J. A.; Goñi-Moreno, A.; de Lorenzo, V. The glycerol-dependent metabolic persistence of *Pseudomonas putida* KT2440 reflects the regulatory logic of the GlpR repressor. *mBio* **2015**, *6*, e00340−15.
(39) Nikel, P. I.; Chavarría, M.; Danchin, A.; de Lorenzo, V. From dirt to industrial applications: *Pseudomonas putida* as a Synthetic Biology *chassis* for hosting harsh biochemical reactions. *Curr. Opin. Chem. Biol.* **2016**, *34*, 20−29.
(40) Nies, S. C.; Alter, T. B.; Nölting, S.; Thiery, S.; Phan, A. N. T.; Drummen, N.; Keasling, J. D.; Blank, L. M.; Ebert, B. E. High titer methyl ketone production with tailored *Pseudomonas taiwanensis* VLB120. *Metab. Eng.* **2020**, *62*, 84−94.
(41) Thorwall, S.; Schwartz, C.; Chartron, J. W.; Wheeldon, I. Stress-tolerant non-conventional microbes enable next-generation chemical biosynthesis. *Nat. Chem. Biol.* **2020**, *16*, 113−121.
(42) Ramos, J. L.; Sol Cuenca, M.; Molina-Santiago, C.; Segura, A.; Duque, E.; Gómez-García, M. R.; Udaondo, Z.; Roca, A. Mechanisms of solvent resistance mediated by interplay of cellular factors in *Pseudomonas putida*. *FEMS Microbiol. Rev.* **2015**, *39*, 555−566.
(43) Sauer, M. Industrial production of acetone and butanol by fermentation—100 years later. *FEMS Microbiol Lett.* **2016**, *363*, fnw134.
(44) Kozaeva, E.; Mol, V.; Nikel, P. I.; Nielsen, A. T. High-throughput colorimetric assays optimized for detection of ketones and aldehydes produced by microbial cell factories. *Microb. Biotechnol.* **2022**, *15*, 2426−2438.
(45) Kozaeva, E.; Nieto-Domínguez, M.; Hernández, A. D.; Nikel, P. I. Synthetic metabolism for *in vitro* acetone biosynthesis driven by ATP regeneration. *RSC Chem. Biol.* **2022**, *3*, 1331−1341.
(46) Yoneda, H.; Tantillo, D. J.; Atsumi, S. Biological production of 2-butanone in *Escherichia coli*. *ChemSusChem* **2014**, *7*, 92−95.
(47) Lan, E. I.; Dekishima, Y.; Chuang, D. S.; Liao, J. C. Metabolic engineering of 2-pentanone synthesis in *Escherichia coli*. *AichE J.* **2013**, *59*, 3167−3175.
(48) Martínez-García, E.; Nikel, P. I.; Aparicio, T.; de Lorenzo, V. *Pseudomonas* 2.0: genetic upgrading of *P. putida* KT2440 as an enhanced host for heterologous gene expression. *Microb. Cell Fact.* **2014**, *13*, 159.
(49) Belda, E.; Van Heck, R. G. A.; López-Sánchez, M. J.; Cruveiller, S.; Barbe, V.; Fraser, C.; Klenk, H.-P.; Petersen, J.; Morgat, A.; Nikel, P. I.; Vallenet, D.; et al. The revisited genome of *Pseudomonas putida* KT2440 enlightens its value as a robust metabolic *chassis*. *Environ. Microbiol.* **2016**, *18*, 3403−3424.
(50) Kozaeva, E.; Volkova, S.; Matos, M. R. A.; Mezzina, M. P.; Wulff, T.; Volke, D. C.; Nielsen, L. K.; Nikel, P. I. Model-guided dynamic control of essential metabolic nodes boosts acetyl-coenzyme A−dependent bioproduction in rewired *Pseudomonas putida*. *Metab. Eng.* **2021**, *67*, 373−386.
(51) Nikel, P. I.; Benedetti, I.; Wirth, N. T.; de Lorenzo, V.; Calles, B. Standardization of regulatory nodes for engineering heterologous

gene expression: a feasibility study. *Microb. Biotechnol.* **2022**, *15*, 2250−2265.
(52) Mezzina, M. P.; Manoli, M. T.; Prieto, M. A.; Nikel, P. I. Engineering native and synthetic pathways in *Pseudomonas putida* for the production of tailored polyhydroxyalkanoates. *Biotechnol. J.* **2021**, *16*, 2000165.
(53) Volke, D. C.; Calero, P.; Nikel, P. I. *Pseudomonas putida*. *Trends Microbiol.* **2020**, *28*, 512−513.
(54) Thompson, M. G.; Incha, M. R.; Pearson, A. N.; Schmidt, M.; Sharpless, W. A.; Eiben, C. B.; Cruz-Morales, P.; Blake-Hedges, J. M.; Liu, Y.; Adams, C. A.; Haushalter, R. W.; et al. Fatty acid and alcohol metabolism in *Pseudomonas putida*: functional analysis using random barcode transposon sequencing. *Appl. Environ. Microbiol.* **2020**, *86*, e01665−20.
(55) Zhang, C.; Yang, H.; Yang, F.; Ma, Y. Current progress on butyric acid production by fermentation. *Curr. Microbiol.* **2009**, *59*, 656−663.
(56) Cerrone, F.; Duane, G.; Casey, E.; Davis, R.; Belton, I.; Kenny, S. T.; Guzik, M. W.; Woods, T.; Babu, R. P.; O'Connor, K. Fed-batch strategies using butyrate for high cell density cultivation of *Pseudomonas putida* and its use as a biocatalyst. *Appl. Microbiol. Biotechnol.* **2014**, *98*, 9217−9228.
(57) Cheung, H. N.; Huang, G. H.; Yu, H. Microbial-growth inhibition during composting of food waste: effects of organic acids. *Bioresour. Technol.* **2010**, *101*, 5925−5934.
(58) Pontrelli, S.; Chiu, T. Y.; Lan, E. I.; Chen, F. Y.; Chang, P.; Liao, J. C. *Escherichia coli* as a host for metabolic engineering. *Metab. Eng.* **2018**, *50*, 16−46.
(59) Park, H.; McGill, S. L.; Arnold, A. D.; Carlson, R. P. Pseudomonad reverse carbon catabolite repression, interspecies metabolite exchange, and consortial division of labor. *Cell. Mol. Life Sci.* **2020**, *77*, 395−413.
(60) Weizmann, C.; Rosenfeld, B. The activation of the butanol-acetone fermentation of carbohydrates by *Clostridium acetobutylicum* (Weizmann). *Biochem. J.* **1937**, *31*, 619−639.
(61) Vögeli, B.; Schulz, L.; Garg, S.; Tarasava, K.; Clomburg, J. M.; Lee, S. H.; Gonnot, A.; Moully, E. H.; Kimmel, B. R.; Tran, L.; Zeleznik, H.; et al. Cell-free prototyping enables implementation of optimized reverse $\beta$-oxidation pathways in heterotrophic and autotrophic bacteria. *Nat. Commun.* **2022**, *13*, 3058.
(62) Favoino, G.; Krink, N.; Schwanemann, T.; Wierckx, N.; Nikel, P. I. Enhanced biosynthesis of poly(3-hydroxybutyrate) in engineered strains of *Pseudomonas putida via* increased malonyl-CoA availability. *Microb. Biotechnol.* **2024**, *17*, e70044.
(63) Silva-Rocha, R.; Martínez-García, E.; Calles, B.; Chavarría, M.; Arce-Rodríguez, A.; de las Heras, A.; Páez-Espino, A. D.; Durante-Rodríguez, G.; Kim, J.; Nikel, P. I.; et al. The Standard European Vector Architecture (SEVA): a coherent platform for the analysis and deployment of complex prokaryotic phenotypes. *Nucleic Acids Res.* **2013**, *41*, D666−D675.
(64) Martínez-García, E.; Fraile, S.; Algar, E.; Aparicio, T.; Velázquez, E.; Calles, B.; Tas, H.; Blázquez, B.; Martín, B.; Prieto, C.; et al. SEVA 4.0: an update of the Standard European Vector Architecture database for advanced analysis and programming of bacterial phenotypes. *Nucleic Acids Res.* **2023**, *51*, D1558−D1567.
(65) Yang, D.; Park, S. Y.; Park, Y. S.; Eun, H.; Lee, S. Y. Metabolic engineering of *Escherichia coli* for natural product biosynthesis. *Trends Biotechnol.* **2020**, *38*, 745−765.
(66) Hartline, C. J.; Schmitz, A. C.; Han, Y.; Zhang, F. Dynamic control in metabolic engineering: theories, tools, and applications. *Metab. Eng.* **2021**, *63*, 126−140.
(67) Orsi, E.; Claassens, N. J.; Nikel, P. I.; Lindner, S. N. Growth-coupled selection of synthetic modules to accelerate cell factory development. *Nat. Commun.* **2021**, *12*, 5295.
(68) Orsi, E.; Claassens, N. J.; Nikel, P. I.; Lindner, S. N. Optimizing microbial networks through metabolic bypasses. *Biotechnol. Adv.* **2022**, *60*, 108035.
(69) Wirth, N. T.; Gurdo, N.; Krink, N.; Vidal-Verdú, A.; Donati, S.; Fernández-Cabezón, L.; Wulff, T.; Nikel, P. I. A synthetic C2 auxotroph of *Pseudomonas putida* for evolutionary engineering of alternative sugar catabolic routes. *Metab. Eng.* **2022**, *74*, 83−97.
(70) Calero, P.; Jensen, S. I.; Nielsen, A. T. Broad-host-range *ProUSER* vectors enable fast characterization of inducible promoters and optimization of *p*-coumaric acid production in *Pseudomonas putida* KT2440. *ACS Synth. Biol.* **2016**, *5*, 741−753.
(71) Gawin, A.; Valla, S.; Brautaset, T. The XylS/*Pm* regulator/promoter system and its use in fundamental studies of bacterial gene expression, recombinant protein production and metabolic engineering. *Microb. Biotechnol.* **2017**, *10*, 702−718.
(72) Krivoruchko, A.; Zhang, Y.; Siewers, V.; Chen, Y.; Nielsen, J. Microbial acetyl-CoA metabolism and metabolic engineering. *Metab. Eng.* **2015**, *28*, 28−42.
(73) Arias-Barrau, E.; Olivera, E. R.; Sandoval, A.; Naharro, G.; Luengo, J. M. Acetyl-CoA synthetase from *Pseudomonas putida* U is the only acyl-CoA activating enzyme induced by acetate in this bacterium. *FEMS Microbiol Lett.* **2006**, *260*, 36−46.
(74) Gardner, J. G.; Escalante-Semerena, J. C. In *Bacillus subtilis*, the sirtuin protein deacetylase, encoded by the *srtN* gene (formerly *yhdZ*), and functions encoded by the *acuABC* genes control the activity of acetyl coenzyme A synthetase. *J. Bacteriol.* **2009**, *191*, 1749−1755.
(75) Sullivan, S. M.; Maddock, J. R. Bacterial division: finding the dividing line. *Curr. Biol.* **2000**, *10*, R249−R252.
(76) Rowlett, V. W.; Margolin, W. The bacterial divisome: ready for its close-up. *Philos. Trans. R. Soc. London B Biol. Sci.* **2015**, *370*, 20150028.
(77) Park, K. T.; Dajkovic, A.; Wissel, M.; Du, S.; Lutkenhaus, J. MinC and FtsZ mutant analysis provides insight into MinC/MinD-mediated *Z* ring disassembly. *J. Biol. Chem.* **2018**, *293*, 5834−5846.
(78) Batianis, C.; Kozaeva, E.; Damalas, S. G.; Martín-Pascual, M.; Volke, D. C.; Nikel, P. I.; Martins dos Santos, V. A. P. An expanded CRISPRi toolbox for tunable control of gene expression in *Pseudomonas putida*. *Microb. Biotechnol.* **2020**, *13*, 368−385.
(79) Jaffé, A.; D'Ari, R.; Hiraga, S. Minicell-forming mutants of *Escherichia coli*: production of minicells and anucleate rods. *J. Bacteriol.* **1988**, *170*, 3094−3101.
(80) Bitzenhofer, N. L.; Höfel, C.; Thies, S.; Weiler, A. J.; Eberlein, C.; Heipieper, H. J.; Batra-Safferling, R.; Sundermeyer, P.; Heidler, T.; Sachse, C.; Busche, T. Exploring engineered vesiculation by *Pseudomonas putida* KT2440 for natural product biosynthesis. *Microb. Biotechnol.* **2024**, *17*, e14312.
(81) Baumgarten, T.; Sperling, S.; Seifert, J.; von Bergen, M.; Steiniger, F.; Wick, L. Y.; Heipieper, H. J. Membrane vesicle formation as a multiple-stress response mechanism enhances *Pseudomonas putida* DOT-T1E cell surface hydrophobicity and biofilm formation. *Appl. Environ. Microbiol.* **2012**, *78*, 6217−6224.
(82) Liao, Y.; Rust, M. J. The Min oscillator defines sites of asymmetric cell division in cyanobacteria during stress recovery. *Cell Syst.* **2018**, *7* (5), 471−481.E6.
(83) Yu, Y.; Zhou, J.; Dempwolff, F.; Baker, J. D.; Kearns, D. B.; Jacobson, S. C. The Min system disassembles FtsZ foci and inhibits polar peptidoglycan remodeling in *Bacillus subtilis*. *mBio* **2020**, *11*, 03197−19.
(84) Männik, J.; Wu, F.; Hol, F. J. H.; Bisicchia, P.; Sherratt, D. J.; Keymer, J. E.; Dekker, C. Robustness and accuracy of cell division in *Escherichia coli* in diverse cell shapes. *Proc. Natl. Acad. Sci. U.S.A.* **2012**, *109*, 6957−6962.
(85) Lin, R.; Deng, C.; Zhang, W.; Hollmann, F.; Murphy, J. D. Production of bio-alkanes from biomass and $CO_2$. *Trends Biotechnol.* **2021**, *39*, 370−380.
(86) Hu, G.; Li, Z.; Ma, D.; Ye, C.; Zhang, L.; Gao, C.; Liu, L.; Chen, X. Light-driven $CO_2$ sequestration in *Escherichia coli* to achieve theoretical yield of chemicals. *Nat. Catal.* **2021**, *4*, 395−406.
(87) Orsi, E.; Nikel, P. I.; Nielsen, L. K.; Donati, S. Synergistic investigation of natural and synthetic C1-trophic microorganisms to foster a circular carbon economy. *Nat. Commun.* **2023**, *14*, 6673.
(88) Orsi, E.; Hernández-Sancho, J. M.; Remeijer, M. S.; Kruis, A. J.; Volke, D. C.; Claassens, N. J.; Paul, C. E.; Bruggeman, F. J.;

Weusthuis, R. A.; Nikel, P. I. Harnessing noncanonical redox cofactors to advance synthetic assimilation of one-carbon feedstocks. *Curr. Opin. Biotechnol.* **2024**, *90*, 103195.
(89) Liew, F. E.; Nogle, R.; Abdalla, T.; Rasor, B. J.; Canter, C.; Jensen, R. O.; Wang, L.; Strutz, J.; Chirania, P.; De Tissera, S.; et al. Carbon-negative production of acetone and isopropanol by gas fermentation at industrial pilot scale. *Nat. Biotechnol.* **2022**, *40*, 335−344.
(90) Poblete-Castro, I.; Wittmann, C.; Nikel, P. I. Biochemistry, genetics, and biotechnology of glycerol utilization in *Pseudomonas* species. *Microb. Biotechnol.* **2020**, *13*, 32−53.
(91) Boecker, S.; Espinel-Ríos, S.; Bettenbrock, K.; Klamt, S. Enabling anaerobic growth of *Escherichia coli* on glycerol in defined minimal medium using acetate as redox sink. *Metab. Eng.* **2022**, *73*, 50−57.
(92) Kim, S. J.; Chang, W.; Oh, M. K. *Escherichia coli* minicells with targeted enzymes as bioreactors for producing toxic compounds. *Metab. Eng.* **2022**, *73*, 214−224.
(93) Kummer, M. J.; Lee, Y. S.; Yuan, M.; Alkotaini, B.; Zhao, J.; Blumenthal, E.; Minteer, S. D. Substrate channeling by a rationally designed fusion protein in a biocatalytic cascade. *JACS Au.* **2021**, *1*, 1187−1197.
(94) Ziegler, A. L.; Grütering, C.; Poduschnick, L.; Mitsos, A.; Blank, L. M. Co-feeding enhances the yield of methyl ketones. *J. Ind. Microbiol. Biotechnol.* **2023**, *50*, kuad029.
(95) Kim, S. J.; Oh, M. K. Minicell-forming *Escherichia coli* mutant with increased chemical production capacity and tolerance to toxic compounds. *Biores. Technol.* **2023**, *371*, 128586.
(96) Elhadi, D.; Lv, L.; Jiang, X. R.; Wu, H.; Chen, G. Q. CRISPRi engineering *E. coli* for morphology diversification. *Metab. Eng.* **2016**, *38*, 358−369.
(97) De Wet, T. J.; Winkler, K. R.; Mhlanga, M.; Mizrahi, V.; Warner, D. F. Arrayed CRISPRi and quantitative imaging describe the morphotypic landscape of essential mycobacterial genes. *eLife* **2020**, *9*, e60083.
(98) Volke, D. C.; Orsi, E.; Nikel, P. I. Emergent CRISPR-Cas-based technologies for engineering non-model bacteria. *Curr. Opin. Microbiol.* **2023**, *75*, 102353.
(99) Dobiašová, H.; Jurkaš, V.; Kabátová, F.; Horvat, M.; Rudroff, F.; Vranková, K.; Both, P.; Winkler, M. Carboligation towards production of hydroxypentanones. *J. Biotechnol.* **2024**, *393*, 161−169.
(100) Hernández-Sancho, J. M.; Boudigou, A.; Alván-Vargas, M. V. G.; Freund, D.; Bååth, J. A.; Westh, P.; Jensen, K.; Noda-García, L.; Volke, D. C.; Nikel, P. I. A versatile microbial platform as a tunable whole-cell chemical sensor. *Nat. Commun.* **2024**, *15*, 8316.
(101) Ali, M. K.; Liu, Q.; Liang, K.; Li, P.; Kong, Q. Bacteria-derived minicells for cancer therapy. *Cancer Lett.* **2020**, *491*, 11−21.
(102) Green, M. R.; Sambrook, J. *Molecular cloning: a laboratory manual*; Cold Spring Harbor Laboratory Press, 2012.
(103) Turlin, J.; Dronsella, B.; De Maria, A.; Lindner, S. N.; Nikel, P. I. Integrated rational and evolutionary engineering of genome-reduced *Pseudomonas putida* strains promotes synthetic formate assimilation. *Metab. Eng.* **2022**, *74*, 191−205.
(104) Kozaeva, E.; Nielsen, Z. S.; Nieto-Domínguez, M.; Nikel, P. I. The pAblo·pCasso self-curing vector toolset for unconstrained cytidine and adenine base-editing in Gram-negative bacteria. *Nucleic Acids Res.* **2024**, *52*, e19.
(105) Ruiz, J. A.; Fernández, R. O.; Nikel, P. I.; Méndez, B. S.; Pettinari, M. J. *dye* (*arc*) Mutants: insights into an unexplained phenotype and its suppression by the synthesis of poly(3-hydroxybutyrate) in *Escherichia coli* recombinants. *FEMS Microbiol Lett.* **2006**, *258*, 55−60.
(106) Nikel, P. I.; Zhu, J.; San, K. Y.; Méndez, B. S.; Bennett, G. N. Metabolic flux analysis of *Escherichia coli creB* and *arcA* mutants reveals shared control of carbon catabolism under microaerobic growth conditions. *J. Bacteriol.* **2009**, *191*, 5538−5548.
(107) Nikel, P. I.; Pettinari, M. J.; Ramírez, M. C.; Galvagno, M. A.; Méndez, B. S. *Escherichia coli arcA* mutants: metabolic profile characterization of microaerobic cultures using glycerol as a carbon source. *J. Mol. Microbiol. Biotechnol.* **2008**, *15*, 48−54.
(108) Fernández-Cabezón, L.; Cros, A.; Nikel, P. I. Spatiotemporal manipulation of the mismatch repair system of *Pseudomonas putida* accelerates phenotype emergence. *ACS Synth. Biol.* **2021**, *10*, 1214−1226.
(109) Wirth, N. T.; Funk, J.; Donati, S.; Nikel, P. I. *QurvE*: user-friendly software for the analysis of biological growth and fluorescence data. *Nat. Protoc.* **2023**, *18*, 2401−2403.
(110) Cavaleiro, A. M.; Kim, S. H.; Seppälä, S.; Nielsen, M. T.; Nørholm, M. H. Accurate DNA assembly and genome engineering with optimized uracil excision cloning. *ACS Synth. Biol.* **2015**, *4*, 1042−1046.
(111) Genee, H. J.; Bonde, M. T.; Bagger, F. O.; Jespersen, J. B.; Sommer, M. O. A.; Wernersson, R.; Olsen, L. R. Software-supported *USER* cloning strategies for site-directed mutagenesis and DNA assembly. *ACS Synth. Biol.* **2015**, *4*, 342−349.
(112) Volke, D. C.; Martino, R. A.; Kozaeva, E.; Smania, A. M.; Nikel, P. I. Modular (de)construction of complex bacterial phenotypes by CRISPR/nCas9-assisted, multiplex cytidine base-editing. *Nat. Commun.* **2022**, *13*, 3026.
(113) Volke, D. C.; Turlin, J.; Mol, V.; Nikel, P. I. Physical decoupling of XylS/*Pm* regulatory elements and conditional proteolysis enable precise control of gene expression in *Pseudomonas putida*. *Microb. Biotechnol.* **2020**, *13*, 222−232.
(114) Pardo, I.; Bednar, D.; Calero, P.; Volke, D. C.; Damborský, J.; Nikel, P. I. A nonconventional Archaeal fluorinase identified by *in silico* mining for enhanced fluorine biocatalysis. *ACS Catal.* **2022**, *12*, 6570−6577.
(115) Lammens, E. M.; Nikel, P. I.; Lavigne, R. Exploring the synthetic biology potential of bacteriophages for engineering non-model bacteria. *Nat. Commun.* **2020**, *11*, 5294.
(116) Nikel, P. I.; Ramirez, M. C.; Pettinari, M. J.; Méndez, B. S.; Galvagno, M. A. Ethanol synthesis from glycerol by *Escherichia coli* redox mutants expressing *adhE* from *Leuconostoc mesenteroides*. *J. Appl. Microbiol.* **2010**, *109*, 492−504.
(117) Wirth, N. T.; Rohr, K.; Danchin, A.; Nikel, P. I. Recursive genome engineering decodes the evolutionary origin of an essential thymidylate kinase activity in *Pseudomonas putida* KT2440. *mBio* **2023**, *14*, e01081−23.
(118) Wirth, N. T.; Nikel, P. I. Combinatorial pathway balancing provides biosynthetic access to 2-fluoro-*cis*,*cis*-muconate in engineered *Pseudomonas putida*. *Chem Catal.* **2021**, *1*, 1234−1259.
(119) Turlin, J.; Puiggené, Ò.; Donati, S.; Wirth, N. T.; Nikel, P. I. Core and auxiliary functions of one-carbon metabolism in *Pseudomonas putida* exposed by a systems-level analysis of transcriptional and physiological responses. *mSystems* **2023**, *8*, e00004−23.
(120) Nikel, P. I.; Chavarría, M.; Martínez-García, E.; Taylor, A. C.; De Lorenzo, V. Accumulation of inorganic polyphosphate enables stress endurance and catalytic vigour in *Pseudomonas putida* KT2440. *Microb. Cell Fact.* **2013**, *12*, 50.
(121) MacDiarmid, J. A.; Mugridge, N. B.; Weiss, J. C.; Phillips, L.; Burn, A. L.; Paulin, R. P.; Haasdyk, J. E.; Dickson, K. A.; Brahmbhatt, V. N.; Pattison, S. T.; James, A. C.; et al. Bacterially derived 400 nm particles for encapsulation and cancer cell targeting of chemotherapeutics. *Cancer Cell* **2007**, *11*, 431−445.
(122) Martínez-García, E.; Fraile, S.; Rodríguez Espeso, D.; Vecchietti, D.; Bertoni, G.; de Lorenzo, V. Naked bacterium: emerging properties of a surfome-streamlined *Pseudomonas putida* strain. *ACS Synth. Biol.* **2020**, *9*, 2477−2492.
(123) Hanahan, D.; Meselson, M. Plasmid screening at high colony density. *Methods Enzymol.* **1983**, *100*, 333−342.
(124) Worsey, M. J.; Williams, P. A. Metabolism of toluene and xylenes by *Pseudomonas putida* (*arvilla*) mt-2: evidence for a new function of the TOL plasmid. *J. Bacteriol.* **1975**, *124*, 7−13.
(125) Bagdasarian, M.; Lurz, R.; Rückert, B.; Franklin, F. C. H.; Bagdasarian, M. M.; Frey, J.; Timmis, K. N. Specific purpose plasmid cloning vectors. II. Broad host range, high copy number, RSF1010-

derived vectors, and a host-vector system for gene cloning in *Pseudomonas*. *Gene* **1981**, *16*, 237−247.
(126) Fernández-Cabezón, L.; Rosich i Bosch, B.; Kozaeva, E.; Gurdo, N.; Nikel, P. I. Dynamic flux regulation for high-titer anthranilate production by plasmid-free, conditionally-auxotrophic strains of *Pseudomonas putida*. *Metab. Eng.* **2022**, *73*, 11−25.
(127) Wirth, N. T.; Kozaeva, E.; Nikel, P. I. Accelerated genome engineering of *Pseudomonas putida* by I-*Sce*I−mediated recombination and CRISPR-Cas9 counterselection. *Microb. Biotechnol.* **2020**, *13*, 233−249.



https://doi.org/10.1021/acssynbio.4c00700
*ACS Synth. Biol.* 2025, 14, 257−272